Dynamic of organic matter and meiofaunal community on a river-dominated shelf (Rhône prodelta, NW Mediterranean Sea): responses to river regime

A.M. Pruski, Jadwiga Rzeznik-Orignac, Philippe Kerhervé, Gilles Vétion, Solveig Bourgeois, Erwan Peru, Pablo Brosset, Flora Toussaint, Christophe Rabouille

Dynamic of organic matter and meiofaunal community on a river-dominated shelf (Rhône prodelta, NW Mediterranean Sea): responses to river regime

Author names and affiliation

Audrey M. Pruski[a], Jadwiga Rzeznik-Orignac[a], Philippe Kerhervé[b], Gilles Vétion[a], Solveig Bourgeois[a], Erwan Peru[a], Pablo Brosset[a], Flora Toussaint[c], Christophe Rabouille[c]

[a] Sorbonne Université, CNRS, Laboratoire d'Ecogéochimie des Environnements Benthiques, LECOB, F-66650 Banyuls-sur-Mer, France

[b] Université de Perpignan Via Domitia, CNRS, Centre de Formation et de Recherche sur les Environnements Méditerranéens, CEFREM, F-66860 Perpignan, France

[c] Laboratoire des Sciences du Climat et de l'Environnement, LSCE/IPSL,CEA-CNRS-UVSQ-Université Paris Saclay, 91198 Gif-sur-Yvette, France

Corresponding author : Audrey M. Pruski, 1 avenue Pierre Fabre, Observatoire Océanologique de Banyuls, 66650 Banyuls sur mer, France

Email : audrey.pruski@obs-banyuls.fr

Tel : 00 33 4 68 88 73 79

Abstract:

In the oligotrophic context of the Mediterranean Sea, riverine inputs of particulate organic matter represent an important source of food for benthic communities. However, since most of these inputs are delivered during short, but intense flood events, communities living in the vicinity of river mouths are also exposed to strong and frequent physical disturbances. A very tight and complex relationship links river dynamic and macrofaunal communities in Mediterranean deltas, but less is known on the response of meiobenthic communities to river regime. In 2010, sediments cores were collected in the Rhône River prodelta in winter and spring before the flooding of the Rhône River tributaries in June, and then twice in the early and late summer. The hypothesis was that increased runoff and export of terrigenous material would induce major changes in the sediment biochemistry, which would in turn trigger modifications in abundances and vertical distribution of the meiofauna. The origin and quality (lability, degradation state) of the different pools of organic matter preserved in these recent sediments were determined using bulk geochemical and molecular analyses (fatty acids, amino acids). Vertical profiles of descriptors for organic matter origin and quality revealed major changes in the nature of the inputs occurring at monthly time scales. Inputs of plant detritus from autumnal and winter flood events were still visible in the cores collected in February and April. A few days after the June 2010 high-discharge event, a newly deposit (~ 7 cm) containing soil organic matter has recovered the prodeltaic sediments and the resident meiofaunal community, but at the end of August only 2 cm of this deposit remained. Multivariate analyses furthermore highlighted that the meiofaunal community was driven by both the trophic conditions and deposition of a new sediment layer driven by the hydrological regime of the Rhône River. In April, increased abundances of meiofauna were observed in response to the sedimentation of labile organic matter after the spring bloom. The June high-discharge event affected the meiofauna with a reduction of its abundance and the burial of the resident meiobenthic community. However, the meiofauna recovered in less than two months after this disturbance, showing the strong resilience of this component of the benthic ecosystem in this high energy environment.

46 **Keywords:** Mediterranean Sea, Rhône River, high-discharge event, physical disturbance, marine
47 sediments, organic matter, meiofauna

1. Introduction

Rivers represent the main source of fresh water, nutrients, sediments and terrestrial organic carbon (OC) to the coastal ocean. Continental shelves influenced by large to medium-sized rivers consequently account for some of the most biologically productive marine systems on Earth and have great ecological, biogeochemical, social and economic values (Day et al., 2019b). River flow dynamic, land use, coastal circulation, resuspension and meteorological events are all parameters that exert some level of control on the delivery and dispersal of riverine inputs of sediments and OC on the shelf. Human activities such as deforestation, agriculture, urbanisation, fluvial regulation and diversion affect the land-ocean export, both quantitatively and qualitatively (Bianchi and Allison, 2009). These transitional areas are also particularly vulnerable to climate-driven disturbances associated with global warming, sea-level rise and the increasing frequency and intensity of storms (O'Leary et al., 2017). How natural and anthropogenic changes in the delivery of terrestrial OC to continental shelves will affect global OC budgets remains largely uncertain (Bauer et al., 2013). Likewise, benthic communities play a central role in the cycling and burial of OC in estuarine ecosystems, but they are particularly exposed to combined anthropogenic stressors (Akoumianaki et al., 2013, 2006; Martin et al., 2019). Given this, the question is how and to what extent, changes in river inputs have an impact on benthic communities and the regulating services they provide.

Deltas are peculiar estuaries that form where sand and mud supply exceeds sediment dispersal. Their existence and functioning are therefore closely linked to river inputs (Giosan et al., 2014). A plethora of river delta systems have formed in the microtidal wave-influenced setting of the Mediterranean Sea (Besset et al., 2017). The watersheds and fluvial regime of most Mediterranean deltas, including the Ebro, Rhône, Po and Nile, have undergone severe modifications to accommodate human activities (Day et al., 2019a). Despite considerable efforts to control the runoff of these rivers, the export of particulate matter takes place primarily during high discharge flood events triggered by intense rainfalls or oceanic storms (Antonelli et al., 2008). Depending on the season and drainage basin affected, the magnitude and nature of the particulate organic matter (POM) exported during these

74 events are highly variable with inputs of fossil OC, eroded soils, riparian vegetation or phytoplankton
75 (Antonelli et al., 2008; Cathalot et al., 2013; Harmelin-Vivien et al., 2010; Higueras et al., 2014; Marion
76 et al., 2010; Tesi et al., 2008). Meteorological and hydrological drivers are thus expected to control the
77 supply and quality of the POM delivered to the shelf as well as its bioavailability for the benthic fauna.
78 Moreover, extreme flooding events results in the rapid deposition of fine terrigenous particles which
79 have significant effects on the structure and function of macrobenthic communities (Cardoso et al.,
80 2008; Lohrer et al., 2004; Norkko et al., 2002). For instance, off the Rhône River, the proliferation of
81 opportunist species taking advantage of flood deposits has been observed in the months following
82 major events (Salen-Picard et al., 2003). A very tight and complex relationship links river dynamic and
83 macrofaunal communities in Mediterranean deltas (Akoumianaki and Nicolaidou, 2007; Bonifácio et al.,
84 2014; Hermand et al., 2008; Salen-Picard et al., 2003). By contrast, meiobenthic communities (animals
85 retained between 40 µm and 1 mm mesh size of sieves; Giere, 2009) from deltaic systems have received
86 little attention (Danovaro et al., 2000; Guidi-Guilvard and Buscail, 1995; Palacín et al., 1992, Semprucci
87 et al., 2019) at the notable exception of foraminiferans (Fontanier et al., 2008; Franzo et al., 2019;
88 Goineau et al., 2012). The meiofauna has an important role in the functioning of benthic ecosystem,
89 contributes significantly to the diet of many other animals (Coull, 1990), and facilitates mineralisation
90 of organic material (Coull, 1999; Gee, 1989; Riera and Hubas, 2003). Because of their small size, lack of
91 larval stage and shorter generation time, meiobenthic organisms respond more successfully than the
92 macrofauna to changes in environmental conditions (Balsamo et al., 2012). As such, meiofaunal
93 communities have been widely used to monitor the effects of both natural and anthropogenic
94 perturbations in aquatic ecosystems (Coull and Chandler, 1992; Gambi et al., 2003; Schratzberger and
95 Ingels, 2018, Semprucci et al., 2018). Although the meiofauna appears as a good bioindicator of organic
96 enrichment and physical disturbance in coastal areas (Gambi et al., 2003), there is a paucity of studies
97 focusing on their response to river inputs (Danovaro et al., 2000; Guidi-Guilvard and Buscail, 1995;
98 Palacín et al., 1992; Pelletier et al., 1999).

In this study, the response of meiofaunal communities to the dynamic of river inputs is discussed. In 2010, we had the opportunity to study the impact of a high-discharge event of the Rhône River, the largest Mediterranean river. Sediments were collected in the winter and spring before this period and afterwards, twice in the early and late summer. The hypothesis was that this extreme event would induce major changes in the sediment biochemistry, which would in turn trigger modifications in abundances and vertical distribution of the meiofauna. The specific aims of the present study were (1) to evaluate how the Rhône River regime affect sediment biochemistry in the prodelta at a seasonal time scale, (2) to investigate whether the main taxa of the meiofauna respond to changes in river inputs, and (3) to determine which of the investigated environmental parameters (i.e. grain-size, porosity, sedimentary organic matter composition, stable isotopic values…) were the most pertinent to illustrate the observed trends. A particular attention was paid at determining the origins and quality of the POM delivered by the Rhône River, as it represents fresh sources of detritus for benthic organisms.

2. Materials and methods

2.1. Regional setting and study area

The Rhône River, now the main river in the Mediterranean Sea since the damming of the Nile, links the Rhône glacier in the Swiss upper Alps to the Camargue delta on the French coast of the Mediterranean Sea (the Gulf of Lion). It is mainly an Alpine river, which drains a relatively small (95,000 km^2), but highly diversified, watershed exhibiting a strong geological heterogeneity (Olivier et al., 2009). The Rhône catchment includes several climatic zones (mountainous, oceanic and Mediterranean) resulting in a very complex hydrological regime and a strong inter annual variability (Pont et al., 2002). Typical of Mediterranean rivers, the runoff of the Rhône is characterised by flooding events triggered by intense rainfalls in autumn and snowmelt in spring. As a consequence, solid export to the Gulf of Lion occurs mainly during short, but intense high-discharge events (Antonelli et al., 2008). Riverine particulate inputs undergo a rapid deposition near the river mouth in the prograding prodelta (Maillet et al., 2006). The unconsolidated sediments are frequently resuspended by episodes of strong winds or

by near bottom currents (Ulses et al., 2008). The study area is located at 2.5 km of the Rhône River mouth in the prodelta area (Fig. 1).

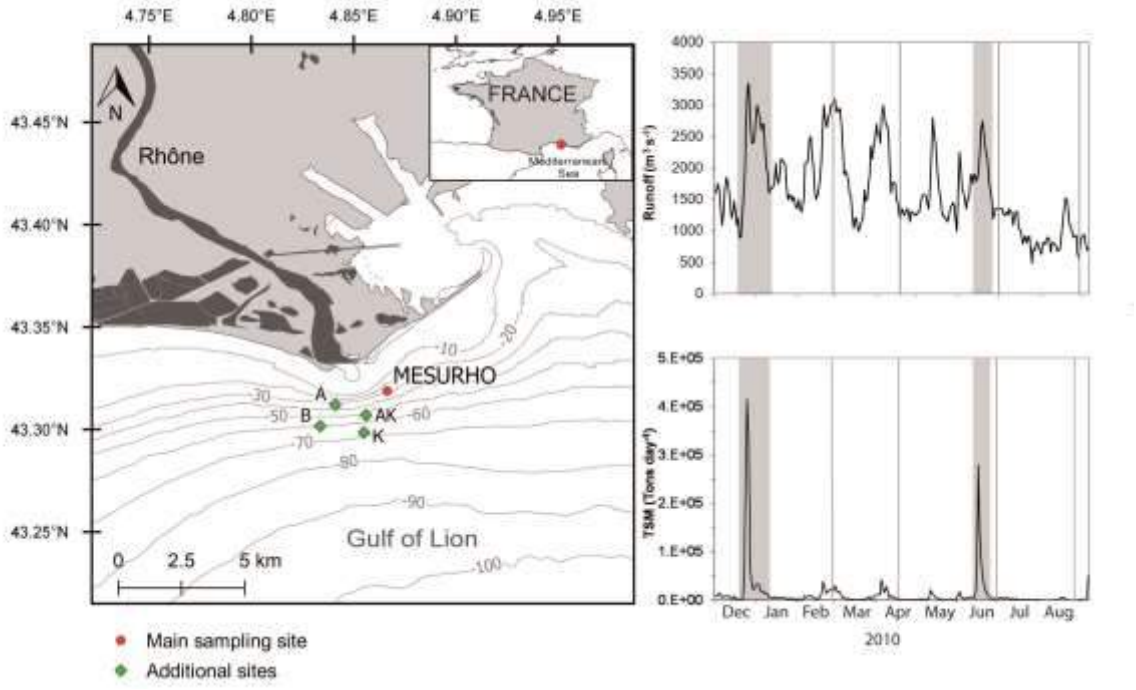

Figure 1: Location of the sampling sites in the Gulf of Lion (left) and Rhône River runoff and total suspended matter (TSM) concentration for 2010 (right). Rhône data were measured at the SORA Observatory Station in Arles, the most downstream gauge station, 40 km upstream the mouth. The vertical bars indicate the sampling dates and the grey areas represent periods of high solid discharge rate.

2.2. Hydrological and climatic conditions

Mean daily discharge data from the Arles gauging station were provided by the CNR (Compagnie Nationale du Rhône, the main hydropower company on the Rhône River). Daily total suspended matter (TSM) concentrations measured in water samples collected at the Rhône observatory station at Arles (SORA) were provided by the MOOSE network (Mediterranean Oceanic Observing System for the Environment – http://www.moose-network.fr). Monthly weather reports were provided by Météo France.

143 2.3. Sediment sampling

144 The sampling targeted four contrasted periods in 2010: winter (20th February), spring (18th
145 April), early (1st July) and late summer (28th August). Sediment cores were collected at station MESURHO
146 (43°19.2 N, 4°52 E, 20 m depth) from the board of the Téthys II R/V using a multicorer MUC 8/100
147 (Oktopus GmbH) during the field campaigns MESURHOBENT 1, 2, 3 and 4 (Rabouille, 2010a, b, c, d). At
148 each sampling date, four undisturbed sediment cores (9.5 cm of diameter and 60 cm of height) were
149 processed on board and sliced into seven horizontal layers (0–0.5, 0.5–1, 1–2, 2–3, 3–5, 5–7 and 7–10
150 cm). Since previous studies in the prodelta area have shown that variability among cores was low
151 (Bourgeois et al., 2011; Cathalot et al., 2010; Pastor et al., 2011a), one core was conditioned in this study
152 for sediment characterisation. Sediment layers were carefully homogenised, distributed in two aliquots
153 and immediately frozen at -20°C. Sediment layers from the three other cores were preserved in 70%
154 alcohol for meiofaunal analysis. Visual observation of the sediment cores used in this study showed no
155 signs of burrows, biogenic structures, oxic voids or large macrofauna, suggesting low bioturbation
156 activity.

157

158 2.4. Assessment of sediment characteristics

159 Sediment granulometry was assessed using a Malvern® Mastersizer 2000 laser diffraction
160 particle size analyser. Porosity (ϕ) was calculated by determining water mass loss during drying
161 assuming a value of 2.63 g.cm^{-3} for grain size density and 1.03 g.cm^{-3} for pore water density. Sediment
162 granulometry, and porosity were determined in triplicate for each sample.

163 Elemental and biochemical analyses were performed on freeze-dried sediments. The analytic
164 protocols for total organic carbon (TOC), bulk stable carbon isotopes ($\delta^{13}C$), total hydrolysable amino
165 acids (THAA) and fatty acids have been described in Fagervold et al. (2014).

166 Enzymatically hydrolysable amino acids (EHAA), which correspond to the fraction of amino acids
167 assumed to be bioavailable for benthic deposit-feeders, were extracted by the biomimetic approach of
168 Mayer et al. (1995). THAAs and EHAAs were analysed by reverse phase high-performance liquid

chromatography (HPLC, Gynkotek-Dionex system) following precolumn derivatisation with orthophtaldialdehyde (Lindroth and Mopper, 1979). The isoindol derivatives were separated on a C18-HPLC column using a non-linear gradient of methanol-acetate buffer and were detected by fluorescence at 450 nm using an excitation wavelength of 335 nm (Bourgeois et al., 2011).

Fatty acid, THAA and EHAA concentrations were normalised to total organic carbon.

2.5. Assessment of meiofaunal abundance and taxonomic composition

The sediment samples were sieved through 1000 and 40 µm mesh simultaneously. The fraction retained on the 40 µm sieve was collected and centrifuged with Ludox HS 40 (density 1.15) as described by Heip et al. (1985). The organisms in the supernatant were collected and rinsed on a 40 µm mesh to remove Ludox and preserved in 70% alcohol. All meiobenthic organisms were counted and classified to higher taxon under a stereomicroscope, after staining with rose Bengal. A sample splitter, Motoda-box (Motoda, 1959) was used to obtain an aliquot containing about 1000 organisms, for the abundance estimations of nematodes and copepods. The number of other meiobenthic taxa was too low to evaluate on split samples, they were thus counted on the whole sample. Total density of meiofauna and of the main representative taxa (nematodes, copepods, annelids, cumaceans, turbellarians, foraminiferans, and kinorhynchs) were determined (number of individuals/10 cm^2) for the four sampling dates. Mean density based on the 3 cores were calculated for each layer. Note that the Ludox extraction is less efficient for organisms with shells, like foraminiferans, molluscs or ostracods, and that the abundances were thus underestimated for these taxa.

2.6. In situ microprofiling of dissolved oxygen and DOU calculation

A benthic lander carrying a benthic microprofiler (Unisense®) was deployed to measure *in situ* microprofiles of dissolved oxygen (Cai and Reimers, 1993; Rabouille et al., 2003; Rassmann et al., 2020 and references therein). The benthic lander was deployed in April, July and August 2010 at a maximum of 5 stations, except in August because of bad weather conditions. These stations encompass the

MESURHO station, another proximal station located in the South of the Rhône River (A), and 3 other stations located in the Rhône prodelta (AK, B and K, Fig. 1).

Four oxygen microelectrodes were simultaneously deployed, and vertical depth profiles were measured with a 200 µm resolution together with a resistivity electrode. As their response to variations in oxygen concentrations is linear (Boudreau and Jorgensen, 2001), the O_2 microelectrodes were calibrated with a two-point calibration technique using the bottom water O_2 concentration determined by Winkler titration and the anoxic pore waters. Signal drift of O_2 microelectrodes during profiling was checked to be less than 5 %. Diffusive oxygen uptake (DOU) rates were calculated using Fick's first law (Berner, 1980, Eq. 3),

$$DOU = -\emptyset \cdot D_s \cdot \left.\frac{d[O_2]}{dz}\right|_{z=0} \qquad (3)$$

where ϕ is sediment porosity, Ds the diffusion coefficient in the sediments ($cm^2\ s^{-1}$), and $\left.\frac{d[O_2]}{dz}\right|_{z=0}$ is the oxygen gradient below the sediment water interface (µmol cm^{-4}). For the calculations, the gradient between 0 and 400 µm in the sediment was consistently used. The Ds coefficients were adjusted for diffusion in a porous environment according to: $D_s = \frac{D_0}{(1+3\cdot(1-\emptyset))}$ with the diffusion coefficient in free water (D_0) taken from Broecker and Peng (1974) and recalculated at *in situ* temperature using Li and Gregory (1974).

2.7. Data analysis

The amount, sources, and quality of the sedimentary organic matter (OM) in the Rhône prodelta were assessed with a suite of bulk and molecular descriptors. The list of the parameters used in this study is provided in Table 1 with their interpretation. The degradation index (DI) was calculated from the molar composition of the THAA hydrolysates (Dauwe et al., 1999a). This index synthesises subtle changes in the amino acid composition linked with diagenesis into a univariate variable indicative of OM degradation stage, whose value decreases with increasing degradation. We applied the same calculation on the EHAA composition of the flood deposit. In this case, the index (DI_{EHAA}) provided information on

220 the degradation stage of the pool of amino acids that may be assimilated by benthic organisms. The
221 reactivity index [RI=(tyrosine+phenylalanine)/(β-alanine+ɣbutyric acid)] is another indicator of OM
222 degradation (Jennerjahn and Ittekkot, 1997). It takes into account two opposite trends: the reactive
223 aromatic amino acids, tyrosine and phenylalanine, are rapidly degraded in decaying OM, whereas their
224 decarboxylation products, β-alanine and ɣ-butyric acid, consistently increase with microbial degradation
225 (Alkhatib et al., 2012; Jennerjahn and Ittekkot, 1997).

226 A one-way ANOVA was used to analyse variations in total meiofaunal abundance whereas two-
227 ways ANOVA were performed to test for differences in meiofaunal vertical distribution with time, with
228 sediment depth and time x sediment depth. Abundances were double square root transformed in order
229 to meet the assumptions for ANOVA (homogeneity of variances, normally distributed residuals). A Tukey
230 Honest Significance Test (HSD) test was applied when significant differences were detected between
231 means. Analyses of variance were run with XLSTAT (V4.01).

232 A principal component analysis (PCA) was then performed to reveal trends in OM composition
233 that could help us retrace the recent history of riverine particle inputs in the prodelta. Prior to PCA, a
234 correlation analysis of the environmental variables was performed to identify variables that were highly
235 correlated, retaining only one of these variables. PCA was combined to hierarchical clustering of the
236 PCA components (HCPC), which determines clusters of samples that present homogenous
237 characteristics (Husson et al., 2010). The HCPC was performed on the 5 first components of the PCA
238 (accounting for 91% of the total variance) using Ward's agglomerative method and a Euclidean distance.
239 PCA and HCPC were performed using R software (3.4.4) with the package 'Rcmdr – Factominer' (Lê et
240 al., 2008).

241 Relationships between the abundance of meiofaunal taxa and factors, representing sediment
242 characteristics, were summarised using a Canonical Correspondence Analysis (CCA) (ter Braak, 1986)
243 performed with the R package 'vegan' (Oksanen et al., 2016). CCA allowed to simultaneously visualise
244 the abundances of the principal meiofaunal taxa, the optimal niches (sample corresponding to sediment
245 depth × date) with the environmental parameters (Borcard et al., 2011). The environmental variables

identified by PCA were first retained. The "vif.cca" function of 'vegan' was then used to identify redundant constraints (i.e. environmental variables with variance inflation factors >10) and were removed from the analysis to reduce collinearity. CCA was finally performed on square root transformed abundances to reduce the weight of abundant taxa and a subset of standardised environmental variables describing the quality of food available for the meiofauna ($\delta^{13}C$, C/N ratio, normalised concentration in EHAA, EHAA/THAA ratio, DI, % Algal PUFA) or related to sediment properties (porosity, % clay, and $CaCO_3$). The statistical significance of the overall relationship and of the canonical axes were evaluated using Monte Carlo permutation tests (999 permutations). The CCA ordination diagram displayed samples and taxa as points and environmental variables as vectors (Borcard et al., 2011). Finally, the relative importance of the explanatory variables was evaluated by forward selection followed by Monte Carlo permutation tests (999 permutations) using the "ordistep" function of 'vegan' (Blanchet et al., 2008). With this method, all variables are ranked on the basis of their marginal effects (i.e. considering each variable as the sole constraining variable) and conditional effects (i.e. forward selection on the best descriptors and evaluation of the fit of each variable in conjunction with the variable(s) already selected).

Result outputs for ANOVA and multivariate analyses are provided in the supplementary material.

3. Results and discussion

3.1. Hydrological and climatological conditions

In 2010, the French Mediterranean coast experienced a cold and rainy winter with strong winds dominated by Mistral. Rains were frequent, but moderate with Rhône water discharge reaching 2500m^3 s^{-1} ten days before February sampling and 3000m^3 s^{-1} on the sampling date (Fig. 1). The organic content of the total suspended matter (TSM) was high (TOC= 7.81% on the 12th of February 2010, Kerhervé unpublished result). March was also rainy and windy. Two minor floods occurred before the April sampling, but TSM only slightly increased during these events. In April, the weather was fair with little

wind and precipitation, but liquid discharge rates were high, possibly because of snow melting. As a consequence, TSM increased above 100mg.L^{-1}. On the 15th and 16th of June 2010, exceptional stormy rains (40cm per day) have generated severe flooding in south-eastern France. This rare and deadly flash flood event is believed to be the most important since 1827 (Payrastre et al., 2012). Rainfalls mostly affected the southeast tributaries of the Rhône River (the Durance, the Buëch, the Verdon, etc.) causing their overflow. The runoff of the Rhône River peaked at 2600$m^3.s^{-1}$, while solid discharge reached 2.8 10^5 tones on June 16, 2010. In the days before return to normal runoff, the Rhône brought approximately one fourth of the annual solid input for 2010. The summer was dry and hot. The daily runoff rate was below the mean inter annual flow rate of 1700 m^3s^{-1} and was typical of low river flow (500-1000 m^3s^{-1}). July was characterised by strong winds generally oriented N-NW (12 to 13 days of Mistral). The wind changed of direction on the 26th of July (S) and generated a storm regime. Meteorological conditions were similar on August with episodes of strong winds.

3.2 Oxygen penetration depth and metabolic activity traced by diffusive oxygen uptake (DOU) in the Rhône prodelta

The oxygen microprofiles recorded *in situ* at station MESURHO display a large decrease below the sediment-water interface over depth of a few millimetres, below which the sediment was completely anoxic (Fig. 2). A clear change in time for the oxygen penetration depth (OPD) is visible on figure 2 with average values of 1.4 ± 0.5 mm in April 2010, 2.6 ± 0.5 mm in July 2010, and 2.4 ± 0.2 mm in August 2010.

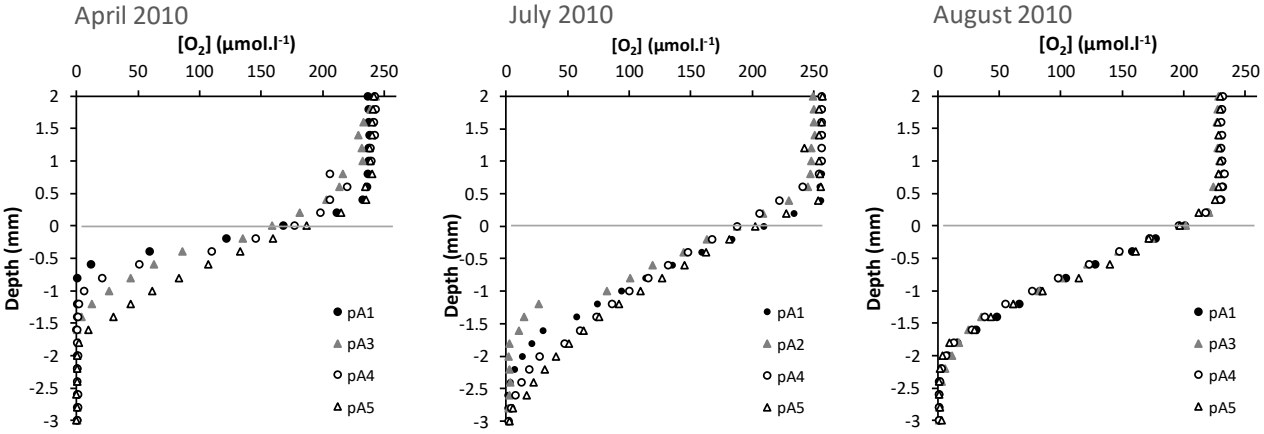

292 **Figure 2: Dissolved oxygen microprofiles at the sediment-water interface recorded *in situ* at the MESURHO**
293 **station in April, July, and August 2010.** Each symbol represents a single electrode profile. The line at 0
294 mm indicates the sediment surface.

295

296 This increase in OPD is accompanied by a decrease of DOU (Table 2), which is a proxy of the metabolic
297 activity in the sediments based on organic matter mineralisation (Cathalot et al., 2010; Rassmann et al.,
298 2020). The DOU recorded at 5 stations in the prodelta show a decrease from April to July, with a levelling
299 in August for the only record that we have at the MESURHO station. The decrease of DOU at the spring-
300 summer transition in 2010 contrasts with the normal spring-summer situation with fresh organic matter
301 deposition and bottom water warming, which generates more mineralisation in surface sediments
302 (Lansard et al., 2008). This unusual decrease in early summer could be related to the high-discharge
303 event in June and the deposition on the seabed of low reactivity material as happened in 2008 during a
304 flood carrying significant amount of material from the Durance tributary (Cathalot et al., 2010). The
305 decrease was more pronounced for stations MESURHO and AK (~ 40% decrease), which are directly
306 under the influence of the Rhône River inputs, and more limited for stations B and K, suggesting lower
307 disturbance with increasing distance from the river mouth.

308

309

3.3. Short-term chronicle of particulate organic matter inputs in the Rhône prodelta

Short sediment cores collected in deltaic areas are useful records of the recent history of riverine POM inputs in coastal areas (Cathalot et al., 2010; Leithold and Hope, 1999). The down-core evolution of sedimentary OM composition provides insights on temporal changes in the characteristics of the POM available for the benthic fauna (Goineau et al., 2012). Clearly, the down-core profiles of organic compounds are far from a textbook situation with steady inputs of OM from the overlying water and progressive degradation on the seafloor (see for instance TOC profiles, Fig. 3). Likewise, descriptors of OM origin ($\delta^{13}C$, fatty acid subgroups) and quality (C/N, EHAA/THAA, DI, RI) point to major changes in the nature of the inputs occurring at a monthly time scale (Fig. 3).

In February, sampling occurred early at the very onset of a Rhône River flood. High organic contents were observed through the sedimentary column, with an integrated TOC content of 1.4% for the ten first centimetres of sediment (Fig. 3). The normalised concentrations in THAA and fatty acids were also high. Descriptors of OM quality and origins revealed strong differences between the surface sediment and the layers below. Phytoplankton markers were only found in the upper layer indicating either the rapid degradation of this labile fraction within the sediments or a recent pulse of POM deriving from microalgae. This assumption is further supported by an enriched $\delta^{13}C$ value as well as by descriptors of OM quality (DI, RI, and EHAA/THAA ratio), which exhibited slightly higher values on the surface than in the layers below (Fig. 3). Subsurface and deeper layers were enriched in coarse material and markers of plant detritus (long chain fatty acids) and had a constant C/N ratio of ~10. These biomarkers associated to high TOC contents and a coarser material are consistent with the preservation of plant detritus brought in autumn and winter.

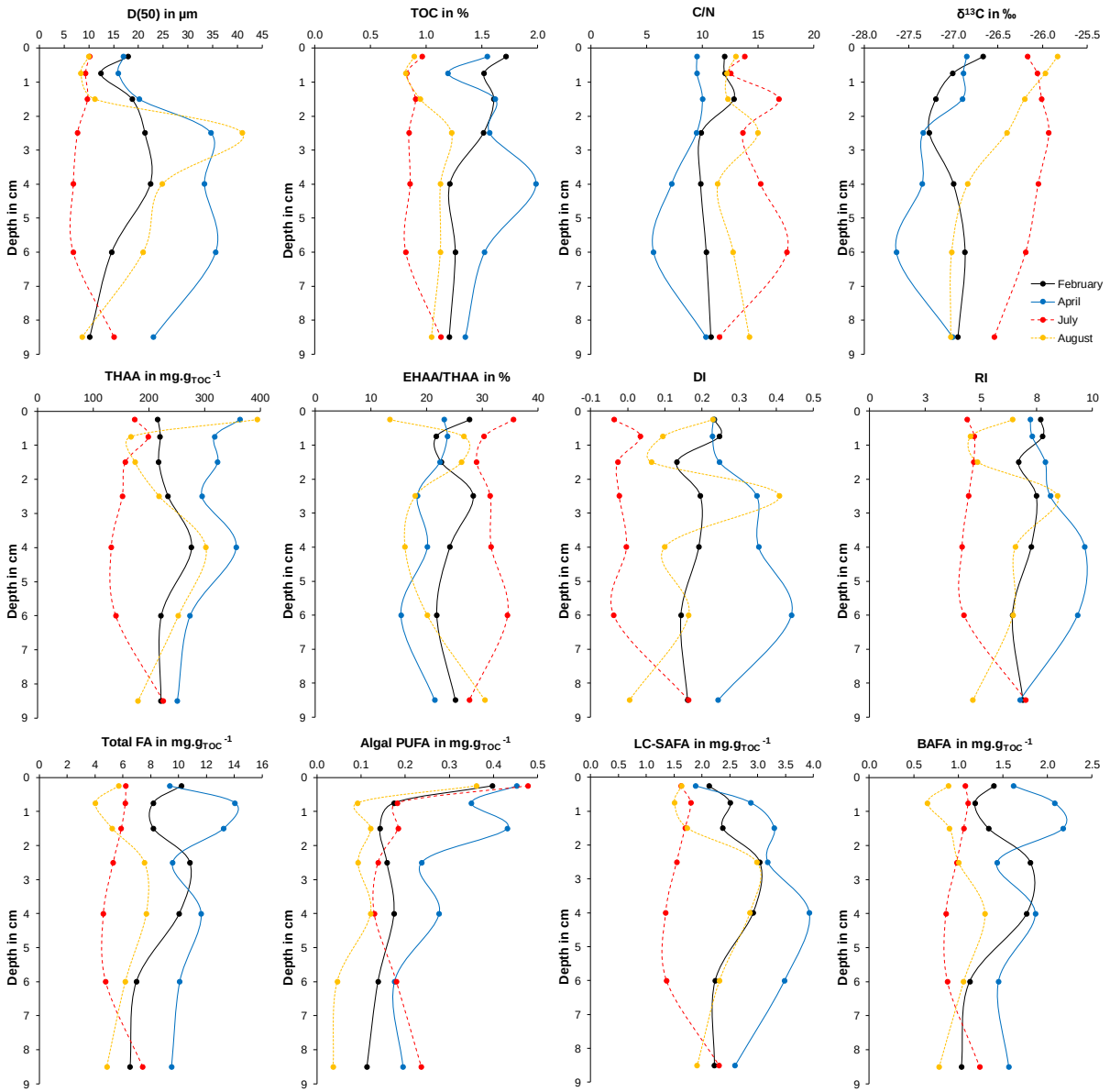

Figure 3: **Down-core evolutions of sediment properties at the MESURHO station in February, April, July, and August 2010.** D(50)= median grain size, TOC= total organic carbon, C/N= molecular carbon to nitrogen ratio, $\delta^{13}C$= bulk stable isotope value, THAA= normalised total hydrolysable amino acid concentration, EHAA/THAA= proportion of enzymatically hydrolysable amino acids, DI= degradation index value, RI= reactivity index, Total FA, Algal PUFA, LC-SAFA and BAFA= TOC-normalised concentrations in total fatty acids, algal polyunsaturated fatty acids, long chain saturated fatty acids and bacterial fatty acids.

In April, sedimentary characteristics were more heterogeneous on the 10cm layer than during the winter (Fig. 3). TOC content was still high and comparable to February in the surface sediment, but

342 at 3-7cm depth, a layer enriched in markers of plant detritus was observed. At the surface, high
343 concentrations in planktonic markers were again suggestive of phytoplankton inputs. Organic carbon,
344 amino acids and fatty acids tended to be higher in the subsurface sediments. This coarser subsurface
345 layer was also less degraded (higher DI and RI) with a lower bioavailability of the amino acid pool.
346 Globally, this suite of descriptors indicates that plant detritus have been exported during the two floods
347 that preceded the sampling, or that earlier deposits in the mud belt have been remobilised. Porosity
348 was also discontinuous, in agreement with the successive deposition of different layers of material.

349 The grain size distribution shows the deposition of about 7 cm of fine particles on the sediment
350 after the torrential rainfalls in June (Fig. 3, 96% of particles <63µm). The sudden peak of TSM (Fig. 1)
351 certainly accounted for this deposit, which was depleted in organic carbon and nitrogen. The flood
352 deposit was also depleted in labile components such as fatty acids and hydrolysable amino acids (on
353 average only ~7% of the TOC was found in the THAA) and was globally more degraded (lower DI and RI)
354 than the material delivered during periods of normal discharge. The characteristics of this fine material
355 recall the one delivered by the Rhône River during the flood of the Durance tributary in June 2008
356 (Bonifácio et al., 2014; Pastor et al., 2018). Following this event, a flood deposit of ~30 cm was observed
357 in the prodelta area (Cathalot et al., 2010). This organic-poor material had a peculiar $\delta^{13}C$ signature (-
358 25.8‰) and displayed a $\Delta^{14}C$ of -495‰ in relation with the refractory nature of the eroded watershed
359 and the flushing of the Serre-Ponçon dam on the Durance (Cathalot et al., 2013; Copard et al., 2018).
360 The decrease in remineralisation activity in the surface sediments after these two events is a further
361 indication that the deposited material was poorly reactive (Table 2).

362 The trend for lower porosities at the end of August suggests that the summer conditions allowed
363 the muddy deposits to settle and become more compact (Table S1, supplementary material). This is
364 consistent with the concomitant stratification of the microbial community described by Fagervold et al.
365 (2014) at this station. Organic content was still low, but OM characteristics indicate intense reworking
366 of the sediments since July (Fig. 3). $\delta^{13}C$ values ranged from "flood signature" of the tributaries (~ -26‰)
367 in surface to the usual winter value of the Rhône (~ -27‰). Below the first two centimetres, which kept

368 the flood imprint, the sediment was enriched in TOC, amino acids, fatty acids, and long chain fatty acids.
369 The down-core evolution of the DI is difficult to interpret. In the surface layer (0-0.5cm), the DI value
370 was similar to values found in February and April on the top of the cores and may be indicative of the
371 recent export of TSM by the Rhône River. Values for the 0.5-1 and 1-2cm layers were closed to those
372 found in the flood deposit, between 2-3cm depth DI was similar to values measured in the April layer
373 enriched with macrodetritus, and below DI was lower indicative of a more degraded pool of POM. Grain
374 size followed the same trend as DI in good consistency with the hypothesis that the 2-3cm layer
375 corresponded to sediments enriched in coarse macrodetritus. The proportion of bioavailable amino
376 acids (EHAA/THAA) was also extremely variable along the sediment depth consistent with inputs of
377 different sources of POM and non-steady state conditions.
378 Taken together all these results show that the flood deposit formed a thinner layer at the end
379 of the summer in comparison to what settled in June. Estimation of the thickness of this layer is about
380 1.5 to 2 cm depending on the parameters used. Compaction cannot entirely account for the reduction
381 of the thickness of the flood deposit. Erosion is the most likely explanation. Strong winds occurred in
382 July (26^{th}) causing the resuspension of sediments at the MESURHO buoy (Lorthiois, 2012). The author
383 described the sediment dynamic during this event as the resuspension of the non-consolidated
384 sediments and their near bottom transport offshore. Dufois et al. (2014) have demonstrated that
385 bottom erosion could be an important process for the sediment dynamic in the prodelta area during
386 moderate river discharge and energetic events. Above the remaining flood deposit, some inputs of fresh
387 suspended particulate matter (DI= 0.23) enriched in labile biogenic compounds (amino acids and fatty
388 acids) have settled during the summer (Fig. 3). Underneath the flood deposit, older consolidated
389 deposits from the autumn, winter and/or spring were found.
390
391
392

3.4. Sources and lability of the sedimentary organic matter in the Rhône prodelta

Down-core evolutions of bulk and molecular descriptors of sedimentary organics in the prodelta highlight the occurrence of several pools of OM, whose dynamic of delivery is related to season and river regime. A PCA was performed to define the biochemical properties of these different pools of OM (Fig. 4).

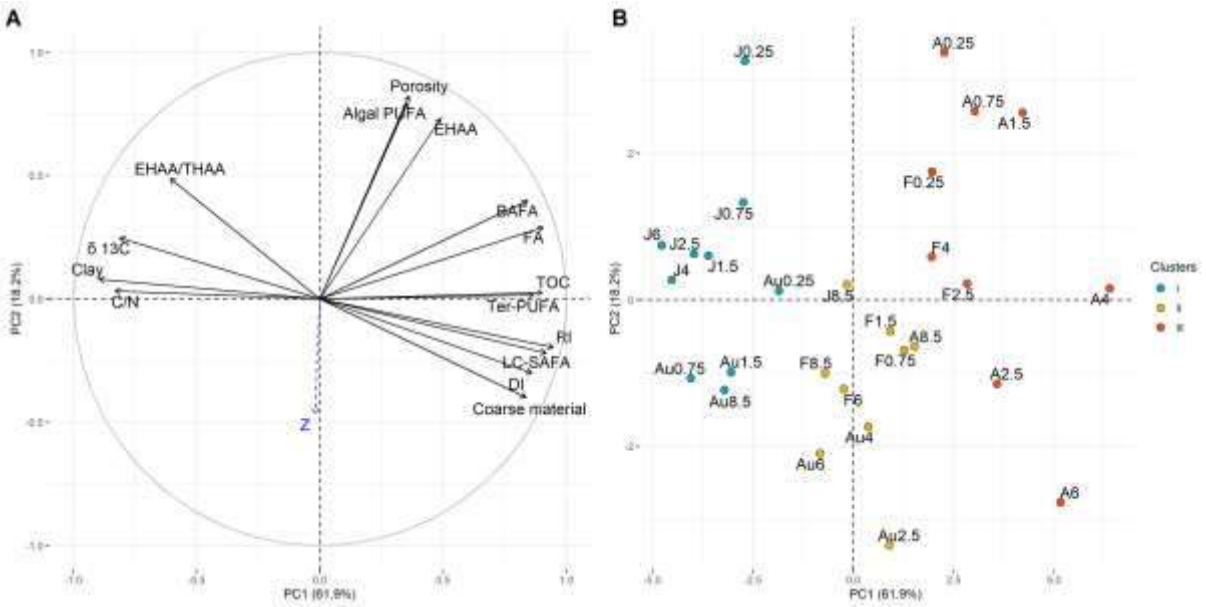

Figure 4: Principal component analysis (PCA) of sediments collected in the Rhône River prodelta: loading plot (A) and score plot (B) for the first and second principal components (7 sediment layers × 4 dates). Black arrows indicate active variables and the blue arrow corresponds to the supplementary variable (sediment depth: Z). Samples were clustered in 3 groups according to a hierarchical clustering analysis performed on the 5 first principal components of the PCA. Sample code is as follow: the letter indicates the month (F= February, A= April, J= July, Au= August) and the number corresponds to the mid-depth of the sediment layer (in cm). Clay= % of particles <4µm, Coarse material= % of particles >200µm, $CaCO_3$ = % of calcium carbonate. For all other variables see Table 1 for abbreviations. Concentrations in EHAA, fatty acids (FA), BAFA, LC-SAFA, Terrestrial PUFA & Algal PUFA were normalised to organic carbon content.

Results of the PCA show that sediment properties can be summarised in two independent principal components explaining 80% of the total variance (Fig. 4A). Sediment layers were not grouped by dates or strata on the two first components of the PCA (Fig. 4B), which is consistent with the

successive deposition of particles originating from different sources. Two pools of organic inputs were clearly separated on the first component axis (PC1= 61.9 % of the total variance). A group of variables with positive loadings on PC1 characterised a coarser material enriched in TOC, fatty acids, and markers of vascular plants (LC-SAFA and Ter PUFA). This material also exhibited higher DI and RI values, indicative of limited diagenetic alteration, and depleted $\delta^{13}C$ values consistent with an input of modern plant detritus in C3 ($\delta^{13}C$ plant = -28‰, Hedges et al., 1986). Taken together, these results confirm that sediment cores collected in February and April 2010 were enriched in plant detritus (Fig. 4B, cluster II). A distinct source of OM associated to clay, low TOC content, higher C/N ratios and $\delta^{13}C$ values was found in June and some sediment layers in August 2010 (negative loadings on PC1 and cluster I). OM in the flood deposit (Cluster I) was also more bioavailable for the benthic fauna as seen by higher EHAA/THAA ratios (Fig. 3). The second principal component (PC2= 18.2% of the total variance) illustrates variations that can be attributed to sediment depth, such as the decrease in porosity in the sedimentary column and the rapid degradation of the most labile components (PUFA deriving from phytoplankton and EHAA). The distribution of layers from the April core along PC2 agrees with this general pattern: the 2 first centimetres (with positive loadings) being enriched in bioavailable OM, whereas the layers below (with negative loadings) contained a more refractory pool of OM. A second group of samples characterised by lower algal contents and porosity was also linked to PC2. This cluster regroups intermediate layers from August and some layers from February (cluster II on Fig. 4B).

The different molecular descriptors used in this study enable to explore the relationships between two fundamental properties of the OM, its origin and its quality. A positive relationship between DI and EHAA/THAA ratio has been previously evidenced supporting the idea that as OM is degraded in the sediments, it becomes less available to enzymes (Dauwe et al., 1999b). Here, the reverse relationship was observed with a significant negative correlation between DI and EHAA/THAA ratio. The mixing of different pools of terrestrial OM may explain these opposite results. A study focusing on the benthic food web in a Mediterranean lagoon has revealed that different types of plants displayed contrasted levels of bioavailability with terrestrial plants exhibiting low EHAA/THAA ratios (10.4-18.1%),

seagrasses having intermediary values (12.2-33.4%), and salt marsh vegetation representing a highly digestive source of OM (50.0-60.2%) (Carlier et al., 2007). In good agreement with these earlier results, macrodetritus isolated from sediments at the MESURHO station have a low digestibility (EHAA/THAA ratio = 9.8) and a DI value (0.29) in the range of those calculated for the layers enriched in plant detritus (Pruski, unpublished result). As a general trend bioavailability was thus higher when the contribution of plant detritus was lower (r^2=0.85). Consequently, the lower bioavailability observed in February, April and some layers from August may be attributed to the presence of macrodetritus. There was also a positive correlation between the DI and the proportion of fatty acids specific of epicuticular waxes from leaves (LC-SAFA) indicating that macrodetritus represent in our system a source of fresh OM, and that LC-SAFA are good tracers of litter inputs (i.e. they are less abundant in soils than in the litter).

In the flood deposit, soils certainly account for most of the particulate OC exported to the prodelta as observed previously after the flood of June 2008 (Cathalot et al., 2013). This hypothesis is supported by low contributions of biomarkers of phytoplankton and higher plant detritus. The different indexes of degradation provide contrasted insights on the history of this material. The low values of the amino acid based degradation indexes (DI and RI) indicate that the POC exported during the June flood was more degraded than the material delivered during periods of normal river regime (Bourgeois et al., 2011). This is consistent with the weathering of degraded POM from soils or riparian areas during intense rainfall events and the decrease of benthic microbial remineralisation (lower DOU in July and August, Table 2). However, the flood deposit was also characterised by high EHAA/THAA ratios (on average 32% in the flood deposit versus 23% in the February and April cores). The higher bioavailability of this material is somewhat counterintuitive. One would expect soil OM to be less prone to enzymatic digestion than fresh detritus. From this point of view, the particulate matter transferred to the sea during the 2008 and 2010 high-discharge events differed remarkably (EHAA/THAA ~20% in 2008, Bonifácio et al., 2014). In 2008, strong rainfalls were responsible for the opening of the spillway of the Serre Ponçon dam (Marion et al., 2010). Silts were eroded from black marls of the Durance watershed. As a consequence, this material was old and refractory ($\Delta^{14}C$= -495.1‰ ± 1.7 in Cathalot et al., 2013;

DI= -0.13, Bourgeois unpublished result). Differences in bioavailability between the TSM delivered during the 2008 and 2010 events may be related to the watersheds affected by the precipitation and the nature of the material transported. Low pigment concentrations in the material exported in June 2010 (Fagervold et al., 2014) indicate that EHAA were mostly associated to non-algal OM, and certainly incorporated to geopolymers as humic substances (Burdige and Martens, 1988). The exported SPM furthermore contained two pools of OM with distinct amino acid compositions: the first and dominant pool was more degraded than the OM delivered during periods of normal discharge (negative DI of the THAAs -0.02±0.03), while another minor fraction of the OM was more labile as shown by elevated DI values calculated on the EHAA (DI_{EHAA} ~0.33± 0.01 for the flood deposit).

3.5. Temporal changes in meiofaunal community

Meiofaunal abundances increased from February (2137 ± 1401 ind. 10 cm^{-2}) to April (9818 ± 2027 ind. 10 cm^{-2}) with intermediate abundances in July (6025 ± 1375 ind. 10 cm^{-2}) and August (4574 ± 1394 ind. 10 cm^{-2}) (Fig. 5). Nematodes were the most abundant metazoans (70%), followed by harpacticoid copepods (18 %), annelids (4.5%), kinorhynchs (4%), foraminiferans (2%), cumaceans (1%) and turbellarians (0.5%) (Supplementary material, Table S2). This community structure was typical of soft bottom habitats (Danovaro et al., 2000; Giere, 2009; Moodley et al., 2000).

Total abundances of meiofauna (Fig. 5) were in the same range as those reported for other sites in the Gulf of Lion (de Bovée et al., 1990; Grémare et al., 2002). Differences between dates were statistically significant (one-way ANOVA, F=15.75, $p < 0.001$). Pairwise comparisons revealed significantly higher abundances in April and significantly lower in February (Tukey post hoc test, Supplementary material, Tables S3 and S4). The fivefold increase in the meiofaunal abundance from February to April coincided with the inputs of fresh and labile OM on the sea floor (enrichment in algal PUFA and amino acids, Fig. 3). Peaks of abundance are frequently observed after the post-bloom sedimentation of phytodetritus (Palacín et al., 1992; Vanaverbeke et al., 2004). Giere (2009) reported

that decaying phytoplankton results in the deposition of a fluffy layer of phytodetritus on the sediment and, after a short time (a few days), those unconsolidated organic deposits enhance the bacterial activity and cause a significant increase in meiofaunal abundance.

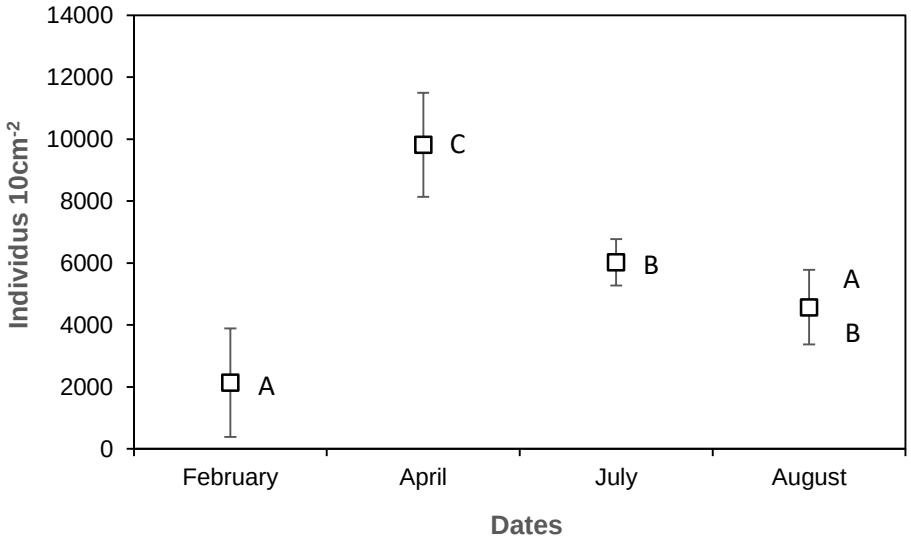

Figure 5: Total meiofaunal abundances at the MESURHO station in February, April, July, and August 2010. Values are means ± SD (n = 3 cores). Analysis of variance (one-way ANOVA, F=15.75, $p < 0.001$) and Tukey post hoc test, dates sharing the same letters are not significantly different.

Results from the two-way ANOVA show the significant effect of sediment depth on the distribution of the meiofauna (F=26.87, $p < 0.001$). Significant "date x sediment depth" interaction terms (F=3.95; $p < 0.001$) furthermore indicate that the vertical distribution of the meiofauna differed between sampling periods (Table S5). In February, April and August, the vertical distribution of the meiofauna showed a typical pattern with high abundances near the surface (0-3 cm depth) and decreasing abundances with sediment depth (Fig. 6) as already described by Soetaert et al. (1995) and Vanreusel et al. (1995). The highest values were recorded on the first 2 cm of the cores, which corresponded to the layers of sediment enriched in phytodetritus (Fig. 3). This vertical pattern could be due to the active migration of the meiofauna to the food source accumulated on the sediment surface (Franco et al., 2008; Moens et al., 2013). Sediment oxygenation could be another regulating factor since

508 oxygen penetration in the sediment was very limited in the prodelta area (Fig. 2). Oxic niches were thus
509 only available close to the sediment–water interface.
510

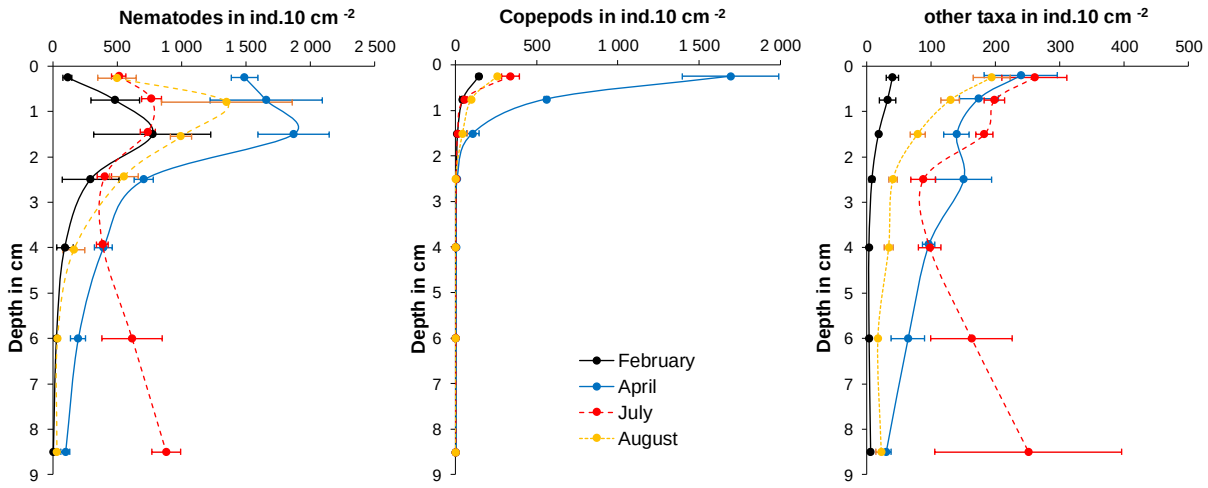

511

512 **Figure 6: Vertical distribution of meiofauna (nematodes, copepods and other taxa) at the MESURHO**
513 **station in February, April, July and August 2010.** Values are means ± SEM (n=3 cores). Note that some
514 symbols were slightly shifted vertically relative to each other for visibility.
515

516 The vertical distribution of the meiofauna in July differed from the general pattern with high
517 abundances in the deep layers similar to those recorded in the very upper layers of the other dates
518 (two-way ANOVA, $p < 0.001$, Supplementary material, Table S5). The vertical profiles of copepods seem
519 to fit the pattern of oxygen penetration depth (Fig. 2), but this clearly does not apply to nematodes and
520 foraminiferans, which displayed the highest abundances in deep sediment layers (5 to 10 cm depth,
521 Supplementary material, Table S2). These changes in the vertical distribution of the main meiofaunal
522 taxa occurred just a couple of days after the flood of the Rhône tributaries and the sudden increase in
523 TSM (Fig. 1). The drop in meiofaunal total abundance and the presence of a high density of nematodes
524 in the deep layers after this high-discharge event can be explained by the burial of the meiobenthic
525 community as observed experimentally with the simulated deposition of dredged material
526 (Schratzberger et al., 2004). As so the present results corroborate the observation of Pelletier (1999)
527 that high-discharge events severely affect the meiofauna with a reduction of its abundance. Among the

528 "other taxa" the clear dominance of foraminifera from genus *Leptohalysis* was noted in July. This
529 foraminiferan is considered as an opportunistic taxon resistant to high turbidity, large inputs of
530 terrestrially-derived OM, and low oxygen penetration in the sediment (Mojtahid et al., 2009; Scott et
531 al., 2005). An opportunistic strategy allows *Leptohalysis* to proliferate in the Rhône prodelta in just a
532 few days after a flood (Goineau et al., 2012).

533 In August, the community had already recovered a pre-disturbance structure. This short
534 resilience time may be explained by a particularity of the study site. The Gulf of Lion is a highly
535 hydrodynamic system, exposed to frequent strong winds and weather conditions where the benthic
536 ecosystem undergoes frequent physical disturbance (Pont et al., 2002). High hydrodynamism can
537 promote meiofaunal recolonisation. Indeed, while strong currents mechanically remove meiofauna
538 from sediment, the first phases of recolonisation generally proceed very rapidly (1-2 weeks) after a
539 severe devastation (review by Coull and Palmer, 1984; Schratzberger et al., 2004). The rapid dispersal
540 of meiofauna has been ascribed primarily to water column processes, including passive erosion or active
541 emergence (Armonies, 1994, 1988; Palmer et al., 1988; Palmer and Gusf, 1985), but the colonisation of
542 defaunated sediments via lateral interstitial migration has also been observed (Schratzberger et al.,
543 2004).

544

545 ### 3.6. Linking meiofaunal composition and sediment properties

546 Canonical correspondence analysis (CCA) allows to relate the abundance of species to
547 environmental variables (ter Braak, 1986). The canonical ordination diagram summarised the ecological
548 preferences of the meiofaunal taxa at the MESURHO station (Fig. 7). This constrained ordination
549 explained 54% of the total inertia. Permutation tests confirmed that relations between taxa abundances
550 and sediment properties were statistically significant (p<0.01) for the sum of all canonical axes (F ratio
551 = 2.3) and for the two first axes (F ratio = 14.9 and 4.2 for axis 1 and axis 2, respectively). Together, the
552 first and second principal canonical axes accounted for 85% of the relationship between taxa and
553 environmental parameters.

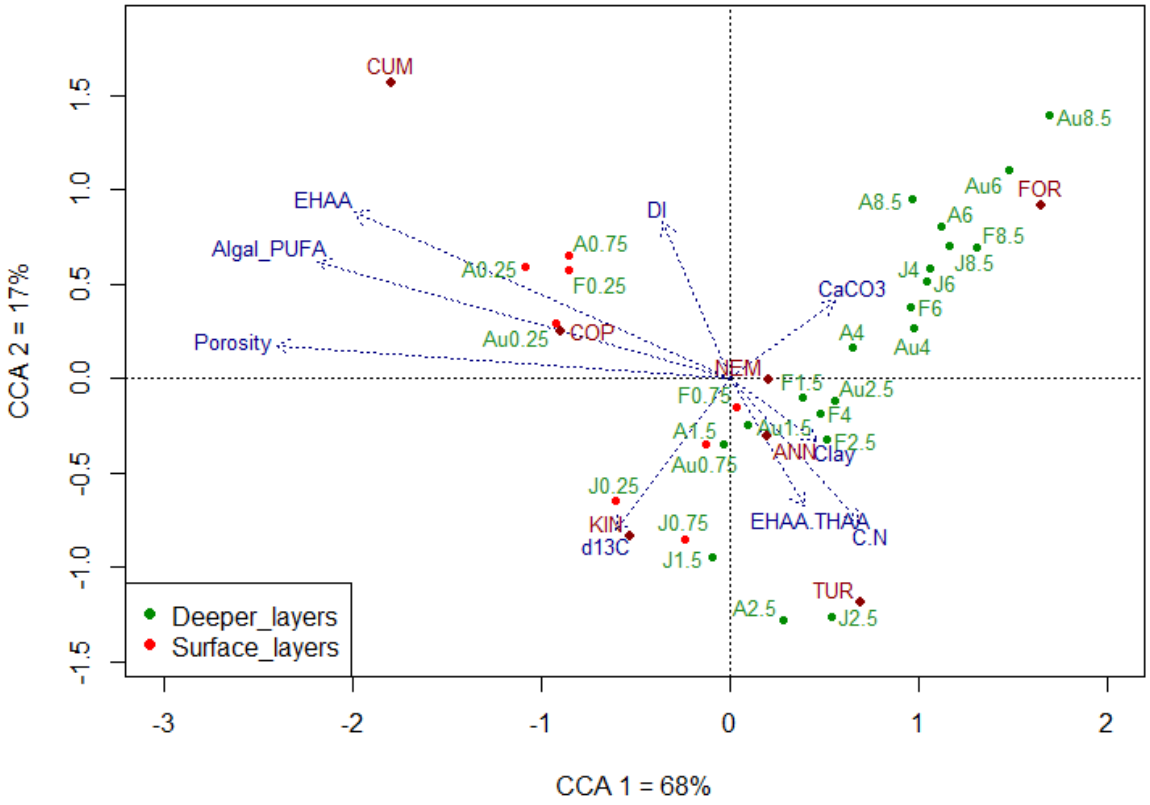

554

555 **Figure 7: Canonical correspondence analysis (CCA) triplot showing ordination of meiofaunal taxa at the**
556 **MESURHO site in February, April, July and August 2010 with environmental variables as arrows and**
557 **samples as dots.**

558 Nematodes (NEM), copepods (COP), kinorhynchs (KIN), annelids (ANN), turbellarians (TUR), cumaceans
559 (CUM), and foraminiferans (FOR). Environmental variables are C/N = molecular carbon to nitrogen ratio,
560 $\delta^{13}C$ = bulk stable isotope value, EHAA: normalised concentration in enzymatically hydrolysable amino
561 acids, EHAA/THAA: enzymatically hydrolysable amino acids to total hydrolysable amino acid ratio, DI=
562 degradation index, algal PUFA = normalised concentration in algal polyunsaturated fatty acids, clay=
563 proportion of clay, $CaCO_3$ = calcium carbonate percentage, and porosity.
564 Sample code is as follow: the letter indicates the month (F= February, A= April, J= July, Au= August) and
565 the number corresponds to the mid-depth of the sediment layer (in cm). Red dots indicate surface
566 sediment layers (0-0.5cm and 0.5-1cm), and green dots deeper sediment layers (1-2cm, 2-3cm, 3-5cm,
567 5-7cm, and 7-10cm).

568

569 Among all the candidate environmental constraints, permutation tests showed that porosity,
570 percentage of algal PUFA and normalised concentration of EHAA were the most influential on the
571 meiofauna (Table 3). These three variables were strongly negatively correlated to the first axis, meaning
572 that the main ecological gradient was linked to higher porosity and inputs of labile OM. DI was positively
573 correlated to the second axis, whereas $\delta^{13}C$, C/N and EHAA/THAA were negatively correlated. With no
574 surprise the meiofaunal community was mainly distributed along the first axis according to sediment
575 depth, with negative scores for the surface layers (0-0.5 & 0.5-1 cm) and positive scores for deeper
576 sediments (below 1cm). The meiofauna inhabiting the surface sediments further aggregated on the
577 second axis according to the origin of the OM. As seen before, in February, April and August, fresh
578 suspended particulate matter settled on the seafloor (Fig. 3). The meiofaunal community clearly
579 responded to these inputs of food with higher frequencies of copepods and cumaceans (Fig. 7). A
580 distinct community was found in July in the three first centimetres of the flood deposit. This community
581 was related to higher $\delta^{13}C$, EHAA/THAA, and C/N ratios. Finally, communities from the deepest sediment
582 layers (5-7 and 7-10cm) were grouped and were not related to any of the environmental factors
583 examined in the present study.
584 The constrained ordination also displayed how the meiofaunal taxa were structured with
585 respect to their environmental constraints and agreed well with the known ecological niches of the
586 recorded taxa. Many cumaceans and harpacticoid copepods rely on planktonic diatoms sinking on the
587 seafloor (De Troch et al., 2005; Giere, 2009; Higgins and Thiel, 1988). In good consistency with their
588 feeding habits, cumaceans and copepods were related to inputs of fatty acids produced by
589 phytoplankton and higher level of bioavailable amino acids found on the top of the cores. Kinorhynchs
590 belong to another group with a known preference for the upper (0-3 cm) oxygenated surface layers
591 (Giere, 2009). Shallow water forms feed mainly on diatoms, but they are also linked to organically
592 enriched sediments (Higgins and Thiel, 1988) as those found near river mouths (Guidi-Guilvard and
593 Buscail, 1995). As expected, kinorhynchs were found in the surface sediments, but they displayed high
594 relative frequencies (~13%) in the flood deposit that recovered the seafloor in July. While kinorhynch

595 density in the top layers remained constant from April to August, copepod and cumacean densities
596 dropped remarkably after the flood (Supplementary material, Table S2). This shows that crustaceans
597 and kinorhynchs respond differently to river regime. In a mesocosm study, Rudnick (1989) found that
598 copepods and kinorhynchs belong to two distinct feeding groups; the first group consuming fresh OM,
599 while the second one could use older detrital matter. However, since the sampling only occurred a few
600 days after the flood, it seems unlikely that the nature of the available OM could be the factor affecting
601 meiofaunal community in July. Kinorhynchs can perform vertical movements in the sediment
602 (Shimanaga et al., 2000). A higher capacity to migrate upward and colonise the newly flood deposit
603 could explain the apparent resilience of kinorhynchs to the physical perturbation induced by the high-
604 discharge event. Nematodes and annelids were the taxa whose occurrence and variability in density
605 were the less explained by the CCA. Free-living nematodes, the metazoans with the greatest species
606 richness in the sediments, occupy various ecological niches with different trophic requirements and
607 sediment preferences (Giere, 2009; Moens et al., 2013), which may explain their wide vertical
608 distribution. The ordination showed anyway their preference for subsurface and deeper sediment
609 layers. Like nematodes, meiobenthic annelids are euryoecious, their preferences relate to sediment
610 structure and organic content (Giere, 2009; Villora-Moreno, 1997). In the present study, they were
611 related to ascending EHAA/THAA and C/N ratios. Foraminiferans were associated with deeper sediment
612 layers and $CaCO_3$. Most foraminiferans are versatile for microhabitat selection, food supply and oxygen
613 availability. Mojtahid et al. (2010) investigated microhabitat preferences of living foraminiferans in front
614 of the Rhône River mouth. They found two different assemblages: infaunal species with maximum
615 densities in anoxic layers were dominant close to the river mouth, while species living predominantly in
616 the top surface layer dominated in areas less influenced by fluvial inputs. They postulated that the
617 higher tolerance of infaunal species for degraded terrestrial OM explains their dominance in the
618 prodelta area. This is consistent with the CCA ordination showing that foraminiferans were related to
619 rather low $\delta^{13}C$ (meaning higher contribution of terrestrial OM). Finally, turbellarians, a group with
620 predatory habits or feeding on diatoms, only occurred in two samples (layers 2-3 cm in April and July).

621 Hence, little can be said of their ecological optimum. However, their occurrence is generally determined
622 by the sediment water and oxygen contents (Giere, 2009).

623 The CCA highlighted that the main ecological gradients for the meiofaunal community in the
624 Rhône prodelta were related to sediment depth and river regime. Strong vertical patterns are found in
625 recent sediments with the degradation of the most labile organic components and short-scale variations
626 of abiotic parameters (oxygenation, redox potential…). These vertical patterns constrain the distribution
627 of the meiofauna (Maria et al., 2012). In contrast, river regime accounts for temporal changes in the
628 amount, provenance and nature of the OM accumulated in the prodelta (Cathalot et al., 2010). The
629 relationships between the meiofauna and the biochemical characteristics of sedimentary OM have been
630 previously investigated by de Bovée et al. (1990) and Grémare et al. (2002) in the Gulf of Lion. They
631 reported that meiofaunal abundance correlated better with concentrations in lipids and EHAA rather
632 than with bulk properties of the OM (nitrogen and organic carbon contents) on the shelf (0 – 175 m
633 depth range). In the present study, porosity, algal PUFA and EHAA were the best predictors of
634 meiofaunal composition, whereas porosity, $\delta^{13}C$ and DI was the best combination of explanatory
635 variables (Table 3). The strong influence of porosity on the meiofauna is certainly indirect. This factor is
636 related to sediment depth as many other environmental variables not measured in the present study.
637 In particular, porosity partially controls important abiotic factors such as dissolved oxygen diffusion and
638 thus redox potential (Eh). The present results furthermore show that qualitative descriptors of
639 sedimentary organics not only explain spatiotemporal changes in meiofaunal composition (de Bovée et
640 al., 1990; Grémare et al., 2002), but also temporal changes in the vertical distribution of meiofaunal
641 taxa.

642

643 4. Conclusions

644 Major variations of the origin and quality of sedimentary OM are observed in the Rhône River
645 prodelta at a monthly time scale. These fluctuations are mainly controlled by the fast dynamic of the
646 processes affecting river flow and inputs from the watershed, but also by biological and physical

processes in the coastal area. Terrestrial organic inputs exported mostly during periods of high river discharge are preserved in the sediments until further remobilisation (Fig. 8). High-discharge events in autumn and winter mostly bring a material enriched in plant detritus, while other events as the one triggered by intense rainfalls in June 2010 are responsible for the transport of more degraded and poorly reactive POC. These different pools of OM (soil, litter, phytodetritus), with variable composition and quality, constitute a variety of trophic resources for the infauna. In this very complex and dynamic system, the meiofaunal community is driven by both trophic conditions and deposition of new sediment layers linked to the hydrological regime of the Rhône River. Inputs of high quality OM (highlighted by fatty acid biomarkers and amino acid indices) appear as a key structuring factor for the meiofauna as already showed by Vanreusel et al. (1995) and Giere (2009). Meiofauna is more abundant in spring when the sedimentation of labile OM originating from the phytoplankton bloom induced eutrophic conditions, whereas meiofaunal densities are low in late summer due to reduced inputs of labile POC (Fig. 8). The current results also point out the rapid response of the meiofauna to a short high-discharge event and the higher importance of analysing the vertical distribution of meiofaunal taxa rather than the total meiofauna abundances, since it was more relevant to show the perturbation. The meiofauna was severely impacted by this physical disturbance with a significant decrease of its total density and the burial of the meiobenthic community under the flood deposit, even though the newly settled layer was rapidly colonised (less than 2 months). The fast recovery of the meiobenthic community highlights that the meiofauna accounts for a highly resilient component of the benthic ecosystem in the vicinity of the Rhône River mouth, in contrast to the macrofauna, which is much longer affected by high-discharge events (Bonifácio et al., 2014).

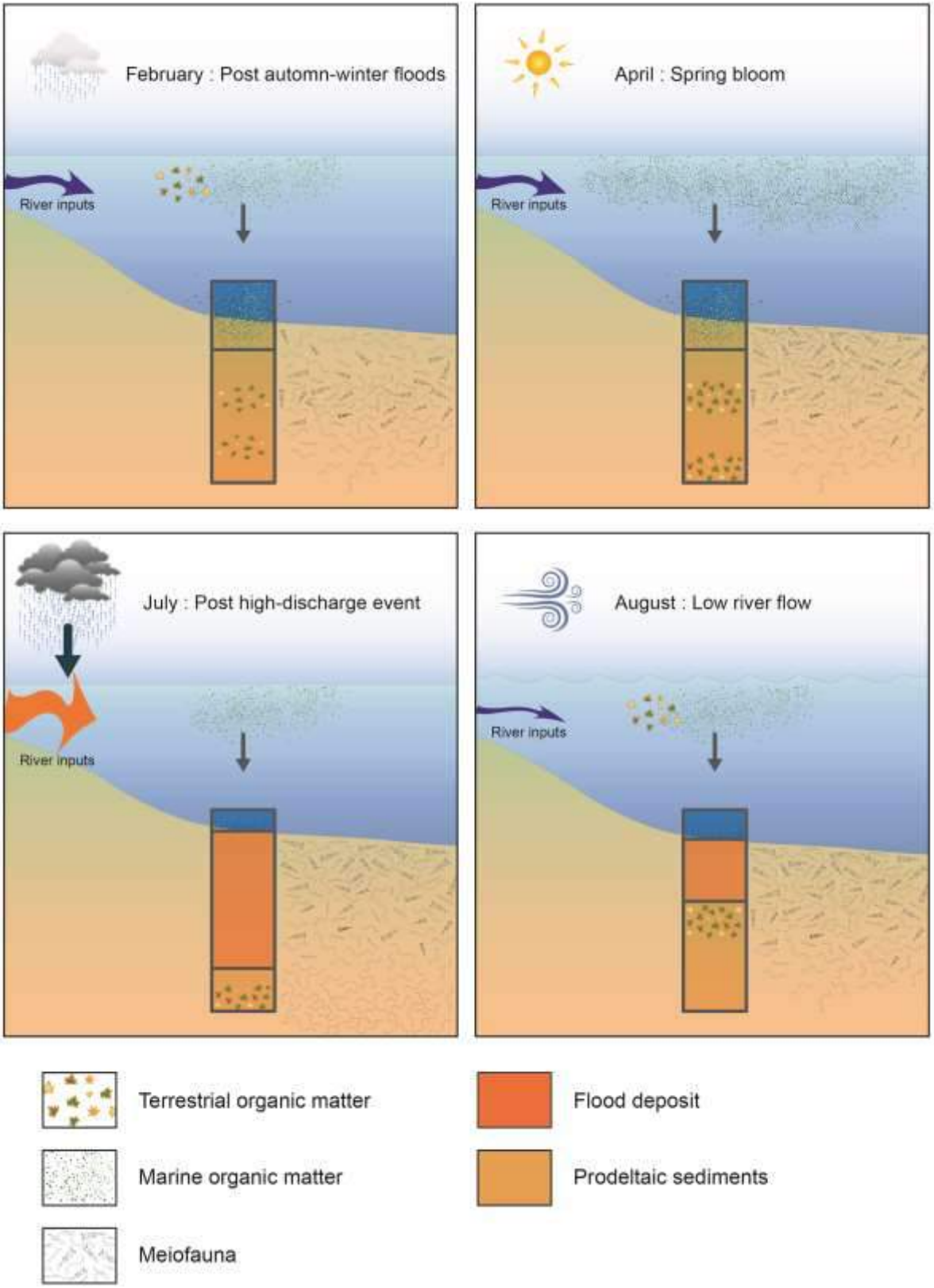

668

669 **Figure 8**: Synthetic scheme of the processes influencing the dynamic of organic matter and meiofaunal
670 community composition during the four investigated periods in the Rhône prodelta.

5. Acknowledgements

This study could not have been conducted without the help of numerous individuals including the captain and crew of the R.V. Tethys II, as well as colleagues from the MESUROBENT group, for their hard work at sea and in the laboratory. We express our sincere gratitude to F. Charles (LECOB) for his help with sediment conditioning on board and B. Bombled (LSCE) who was in charge of the multicorer. We thank L. Feuillassier (LECOB) for his help with grain size analyses, K. Escoubeyrou (OOB) for her help with HPLC analyses and G. Genty (CEFREM) for the elemental analyses. Special thanks to V. Domien (OOB) for her art work on the graphical abstract and Figure 8. S.B. was supported by a Ph.D. scholarship from the French ministry of research and education. This research was funded by the French program MISTRALS/MERMEX, the CNRS, and the UPMC.

682 References

683 Akoumianaki, I., Nicolaidou, A., 2007. Spatial variability and dynamics of macrobenthos in a
684 Mediterranean delta front area: The role of physical processes. Journal of Sea Research 57, 47–
685 64. https://doi.org/10.1016/j.seares.2006.07.003

686 Akoumianaki, I., Papaspyrou, S., Kormas, K.Ar., Nicolaidou, A., 2013. Environmental variation and
687 macrofauna response in a coastal area influenced by land runoff. Estuarine, Coastal and Shelf
688 Science, Estuarine and lagoon biodiversity and their natural goods and services 132, 34–44.
689 https://doi.org/10.1016/j.ecss.2012.04.009

690 Akoumianaki, I., Papaspyrou, S., Nicolaidou, A., 2006. Dynamics of macrofaunal body size in a deltaic
691 environment. Marine Ecology Progress Series 321, 55–66.
692 https://doi.org/10.3354/meps321055

693 Alkhatib, M., Schubert, C.J., del Giorgio, P.A., Gélinas, Y., Lehmann, M.F., 2012. Organic matter reactivity
694 indicators in sediments of the St. Lawrence Estuary. Estuarine, Coastal and Shelf Science 102–
695 103, 36–47. https://doi.org/10.1016/j.ecss.2012.03.002

696 Antonelli, C., Eyrolle, F., Rolland, B., Provansal, M., Sabatier, F., 2008. Suspended sediment and 137Cs
697 fluxes during the exceptional December 2003 flood in the Rhône River, southeast France.
698 Geomorphology 95, 350–360. https://doi.org/10.1016/j.geomorph.2007.06.007

699 Armonies, W., 1994. Drifting meio- and macrobenthic invertebrates on tidal flats in Königshafen: A
700 review. Helgolander Meeresunters 48, 299–320. https://doi.org/10.1007/BF02367043

701 Armonies, W., 1988. Active emergence of meiofauna from intertidal sediment. Marine Ecology Progress
702 Series 43, 151–159. https://doi.org/10.3354/meps043151

703 Balsamo, M., Semprucci, F., Frontalini, F., Coccioni, R., 2012. Meiofauna as a tool for marine ecosystem
704 biomonitoring, in: Marine Ecosystems. In Tech, pp. 77–104. https://doi.org/10.5772/34423

705 Bauer, J.E., Cai, W.-J., Raymond, P.A., Bianchi, T.S., Hopkinson, C.S., Regnier, P.A.G., 2013. The changing
706 carbon cycle of the coastal ocean. Nature 504, 61–70. https://doi.org/10.1038/nature12857

707 Berner, R.A., 1980. Early diagenesis: A theoretical approach. Princeton Univ Pr.

Besset, M., Anthony, E.J., Sabatier, F., 2017. River delta shoreline reworking and erosion in the Mediterranean and Black Seas: the potential roles of fluvial sediment starvation and other factors. Elementa: Science of the Anthropocene 5, 54. https://doi.org/10.1525/elementa.139

Bianchi, T.S., Allison, M.A., 2009. Large-river delta-front estuaries as natural "recorders" of global environmental change. Proceedings of the National Academy of Sciences 106, 8085–8092. https://doi.org/10.1073/pnas.0812878106

Bianchi, T.S., Canuel, E.A., 2011. Chapter 2. Chemical biomarkers applications to ecology and paleoecology, in: Chemical Biomarkers in Aquatic Ecosystems. Princeton University Press, pp. 19–29.

Blanchet, F.G., Legendre, P., Borcard, D., 2008. Forward selection of explanatory variables. Ecology 89, 2623–2632. https://doi.org/10.1890/07-0986.1

Bonifácio, P., Bourgeois, S., Labrune, C., Amouroux, J.M., Escoubeyrou, K., Buscail, R., Romero-Ramirez, A., Lantoine, F., Vétion, G., Bichon, S., Desmalades, M., Rivière, B., Deflandre, B., Grémare, A., 2014. Spatiotemporal changes in surface sediment characteristics and benthic macrofauna composition off the Rhône River in relation to its hydrological regime. Estuarine, Coastal and Shelf Science 151, 196–209. https://doi.org/10.1016/j.ecss.2014.10.011

Borcard, D., Gillet, F., Legendre, P., 2011. Numerical ecology with R, Use R! Springer, New York.

Boudreau, B.P., Jorgensen, B.B., 2001. The Benthic boundary layer: transport processes and biogeochemistry. Oxford University Press.

Bourgeois, S., Pruski, A.M., Sun, M.-Y., Buscail, R., Lantoine, F., Kerhervé, P., Vétion, G., Rivière, B., Charles, F., 2011. Distribution and lability of land-derived organic matter in the surface sediments of the Rhône prodelta and the adjacent shelf (Mediterranean Sea, France): a multi proxy study. Biogeosciences 8, 3107–3125. https://doi.org/10.5194/bg-8-3107-2011

Broecker, W., Peng, T., 1974. Gas-Exchange Rates Between Air and Sea. Tellus 26, 21–35. https://doi.org/10.1111/j.2153-3490.1974.tb01948.x

733 Budge, S.M., Parrish, C.C., McKenzie, C.H., 2001. Fatty acid composition of phytoplankton, settling
734 particulate matter and sediments at a sheltered bivalve aquaculture site. Marine Chemistry 76,
735 285–303.
736 Burdige, D.J., Martens, C.S., 1988. Biogeochemical cycling in an organic-rich coastal marine basin: 10.
737 The role of amino acids in sedimentary carbon and nitrogen cycling. Geochimica et
738 Cosmochimica Acta 52, 1571–1584. https://doi.org/10.1016/0016-7037(88)90226-8
739 Cai, W., Reimers, C., 1993. The Development of Ph and Pco2 Microelectrodes for Studying the Carbonate
740 Chemistry of Pore Waters Near the Sediment-Water Interface. Limnol. Oceanogr. 38, 1762–
741 1773. https://doi.org/10.4319/lo.1993.38.8.1762
742 Cardoso, P.G., Raffaelli, D., Lillebø, A.I., Verdelhos, T., Pardal, M.A., 2008. The impact of extreme flooding
743 events and anthropogenic stressors on the macrobenthic communities' dynamics. Estuarine,
744 Coastal and Shelf Science, Submarine groundwater discharge studies along the Ubatuba coastal
745 area in south-eastern Brazil 76, 553–565. https://doi.org/10.1016/j.ecss.2007.07.026
746 Carlier, A., Riera, P., Amouroux, J.-M., Bodiou, J.-Y., Escoubeyrou, K., Desmalades, M., Caparros, J.,
747 Grémare, A., 2007. A seasonal survey of the food web in the Lapalme Lagoon (northwestern
748 Mediterranean) assessed by carbon and nitrogen stable isotope analysis. Estuarine, Coastal and
749 Shelf Science 73, 299–315. https://doi.org/10.1016/j.ecss.2007.01.012
750 Cathalot, C., Rabouille, C., Pastor, L., Deflandre, B., Viollier, E., Buscail, R., Grémare, A., Treignier, C.,
751 Pruski, A., 2010. Temporal variability of carbon recycling in coastal sediments influenced by
752 rivers: assessing the impact of flood inputs in the Rhône River prodelta. Biogeosciences 7, 1187–
753 1205.
754 Cathalot, C., Rabouille, C., Tisnerat-Laborde, N., Toussaint, F., Kerherve, P., Buscail, R., Loftis, K., Sun, M.-
755 Y., Tronczynski, J., Azoury, S., Lansard, B., Treignier, C., Pastor, L., Tesi, T., 2013. The fate of river
756 organic carbon in coastal areas: A study in the Rhone River delta using multiple isotopic (delta
757 C-13, Delta C-14) and organic tracers. Geochimica et Cosmochimica Acta 118, 33–55.
758 https://doi.org/10.1016/j.gca.2013.05.001

759 Copard, Y., Eyrolle, F., Radakovitch, O., Poirel, A., Raimbault, P., Gairoard, S., Di-Giovanni, C., 2018.
760 Badlands as a hot spot of petrogenic contribution to riverine particulate organic carbon to the
761 Gulf of Lion (NW Mediterranean Sea). Earth Surface Processes and Landforms 43, 2495–2509.
762 https://doi.org/10.1002/esp.4409
763 Coull, B.C., 1999. Role of meiofauna in estuarine soft-bottom habitats. Austral Ecology 24, 327–343.
764 https://doi.org/10.1046/j.1442-9993.1999.00979.x
765 Coull, B.C., 1990. Are Members of the Meiofauna Food for Higher Trophic Levels? Transactions of the
766 American Microscopical Society 109, 233–246. https://doi.org/10.2307/3226794
767 Coull, B.C., Chandler, G.T., 1992. Pollution and meiofauna: field, laboratory, and mesocosm studies.
768 Oceanography and Marine Biology: An Annual Review 30, 191–271.
769 Coull, B.C., Palmer, M.A., 1984. Field experimentation in meiofaunal ecology. Hydrobiologia 118, 1–19.
770 https://doi.org/10.1007/BF00031783
771 Danovaro, R., Gambi, C., Manini, E., Fabiano, M., 2000. Meiofauna response to a dynamic river plume
772 front. Marine Biology 137, 359–370. https://doi.org/10.1007/s002270000353
773 Dauwe, B., Middelburg, J.J., Herman, P.M.J., Heip, C.H.R., 1999a. Linking diagenetic alteration of amino
774 acids and bulk organic matter reactivity. Limnology and Oceanography 44, 1809–1814.
775 Dauwe, B., Middelburg, J.J., Van Rijswijk, P., Sinke, J., Herman, P.M.J., Heip, C.H.R., 1999b. Enzymatically
776 hydrolyzable amino acids in North Sea sediments and their possible implication for sediment
777 nutritional values. Journal of Marine Research 57, 109–134.
778 Day, J.W., Ibáñez, C., Pont, D., Scarton, F., 2019a. Chapter 14 - Status and Sustainability of
779 Mediterranean Deltas: The Case of the Ebro, Rhône, and Po Deltas and Venice Lagoon, in:
780 Wolanski, E., Day, J.W., Elliott, M., Ramachandran, R. (Eds.), Coasts and Estuaries. Elsevier, pp.
781 237–249. https://doi.org/10.1016/B978-0-12-814003-1.00014-9
782 Day, J.W., Ramachandran, R., Giosan, L., Syvitski, J., Paul Kemp, G., 2019b. Chapter 9 - Delta Winners
783 and Losers in the Anthropocene, in: Wolanski, E., Day, J.W., Elliott, M., Ramachandran, R. (Eds.),

784 Coasts and Estuaries. Elsevier, pp. 149–165. https://doi.org/10.1016/B978-0-12-814003-
785 1.00009-5
786 de Bovée, F., Guidi, L.D., Soyer, J., 1990. Quantitative distribution of deep-sea meiobenthos in the
787 northwestern Mediterranean (Gulf of Lions). Continental Shelf Research 10, 1123–1145.
788 https://doi.org/10.1016/0278-4343(90)90077-Y
789 De Troch, M., Steinarsdottir, M., Chepurnov, V., Olafsson, E., 2005. Grazing on diatoms by harpacticoid
790 copepods: species-specific density-dependent uptake and microbial gardening. Aquatic
791 Microbial Ecology 39, 135–144.
792 Dufois, F., Verney, R., Le Hir, P., Dumas, F., Charmasson, S., 2014. Impact of winter storms on sediment
793 erosion in the Rhone River prodelta and fate of sediment in the Gulf of Lions (North Western
794 Mediterranean Sea). Continental Shelf Research 72, 57–72.
795 https://doi.org/10.1016/j.csr.2013.11.004
796 Dunstan, G.A., Volkman, J.K., Barrett, S.M., Leroi, J.M., Jeffrey, S.W., 1994. Essential polyunsaturated
797 fatty acids from 14 species of diatom (Bacillariophyceae). Phytochemistry 35, 155–161.
798 Fagervold, S.K., Bourgeois, S., Pruski, A.M., Charles, F., Kerhervé, P., Vetion, G., Galand, P.E., 2014. River
799 organic matter shapes microbial communities in the sediment of the Rhône prodelta. The ISME
800 journal. https://doi.org/10.1038/ismej.2014.86
801 Fontanier, C., Jorissen, F., Lansard, B., Mouret, A., Buscail, R., Schmidt, S., Kerherve, P., Buron, F.,
802 Zaragosi, S., Hunault, G., Ernoult, E., Artero, C., Anschutz, P., Rabouille, C., 2008. Live
803 foraminifera from the open slope between Grand Rhone and Petit Rhone Canyons (Gulf of Lions,
804 NW Mediterranean). Deep Sea Research Part I: Oceanographic Research Papers 55, 1532–1553.
805 https://doi.org/10.1016/j.dsr.2008.07.003
806 Franco, M.A., Soetaert, K., Oevelen, D.V., Gansbeke, D.V., Costa, M.J., Vincx, M., Vanaverbeke, J., 2008.
807 Density, vertical distribution and trophic responses of metazoan meiobenthos to phytoplankton
808 deposition in contrasting sediment types. Marine Ecology Progress Series 358, 51–62.
809 https://doi.org/10.3354/meps07361

Franzo, A., Asioli, A., Roscioli, C., Patrolecco, L., Bazzaro, M., Del Negro, P., Cibic, T., 2019. Influence of natural and anthropogenic disturbances on foraminifera and free-living nematodes in four lagoons of the Po delta system. Estuarine, Coastal and Shelf Science 220, 99–110. https://doi.org/10.1016/j.ecss.2019.02.039

Gambi, C., Totti, C., Manini, E., 2003. Impact of Organic Loads and Environmental Gradients on Microphytobenthos and Meiofaunal Distribution in a Coastal Lagoon. Chemistry and Ecology 19, 207–223. https://doi.org/10.1080/0275754031000119951

Gee, J.M., 1989. An ecological and economic review of meiofauna as food for fish. Zoological Journal of The Linnean Society 96, 243–261. https://doi.org/10.1111/j.1096-3642.1989.tb02259.x

Giere, O., 2009. Meiobenthology: The Microscopic Motile Fauna of Aquatic Sediments, 2nd ed. Springer-Verlag, Berlin Heidelberg. https://doi.org/10.1007/978-3-540-68661-3

Giosan, L., Syvitski, J., Constantinescu, S., Day, J., 2014. Climate change: Protect the world's deltas. Nature News 516, 31. https://doi.org/10.1038/516031a

Goineau, A., Fontanier, C., Jorissen, F., Buscail, R., Kerherve, P., Cathalot, C., Pruski, A.M., Lantoine, F., Bourgeois, S., Metzger, E., Legrand, E., Rabouille, C., 2012. Temporal variability of live (stained) benthic foraminiferal faunas in a river-dominated shelf - Faunal response to rapid changes of the river influence (Rhone prodelta, NW Mediterranean). Biogeosciences 9, 1367–1388. https://doi.org/10.5194/bg-9-1367-2012

Grémare, A., Medernach, L., deBovee, F., Amouroux, J.M., Vetion, G., Albert, P., 2002. Relationships between sedimentary organics and benthic meiofauna on the continental shelf and the upper slope of the Gulf of Lions (NW Mediterranean). Marine Ecology Progress Series 234, 85–94.

Guidi-Guilvard, L.D., Buscail, R., 1995. Seasonal survey of metazoan meiofauna and surface sediment organics in a non-tidal turbulent sublittoral prodelta (northwestern Mediterranean). Continental Shelf Research 15, 633–653. https://doi.org/10.1016/0278-4343(94)E0036-L

834 Harmelin-Vivien, M., Dierking, J., Bănaru, D., Fontaine, M.F., Arlhac, D., 2010. Seasonal variation in stable
835 C and N isotope ratios of the Rhone River inputs to the Mediterranean Sea (2004–2005).
836 Biogeochemistry 100, 139–150. https://doi.org/10.1007/s10533-010-9411-z
837 Harmelin-Vivien, M., Loizeau, V., Mellon, C., Beker, B., Arlhac, D., Bodiguel, X., Ferraton, F., Hermand,
838 R., Philippon, X., Salen-Picard, C., 2008. Comparison of C and N stable isotope ratios between
839 surface particulate organic matter and microphytoplankton in the Gulf of Lions (NW
840 Mediterranean). Continental Shelf Research 28, 1911–1919.
841 https://doi.org/10.1016/j.csr.2008.03.002
842 Hedges, J.I., Clark, W.A., Quay, P.D., Richey, J.E., Devol, A.H., Santos, U. de M., 1986. Compositions and
843 fluxes of particulate organic material in the Amazon River. Limnology and Oceanography 31,
844 717–738.
845 Hedges, J.I., Oades, J.M., 1997. Comparative organic geochemistries of soils and marine sediments.
846 Organic Geochemistry 27, 319–361. https://doi.org/10.1016/S0146-6380(97)00056-9
847 Heip, C.H.R., Vincx, M., Vranken, G., 1985. The ecology of marine nematodes. Oceanography and Marine
848 Biology: An Annual Review.
849 Hermand, R., Salen-Picard, C., Alliot, E., Degiovanni, C., 2008. Macrofaunal density, biomass and
850 composition of estuarine sediments and their relationship to the river plume of the Rhône River
851 (NW Mediterranean). Estuarine, Coastal and Shelf Science 79, 367–376.
852 Higgins, R.P., Thiel, H., 1988. Introduction to the study of meiofauna, illustrée, révisée, réimprimée. ed.
853 Smithsonian Institution Press, University of Maine.
854 Higueras, M., Kerhervé, P., Sanchez-Vidal, A., Calafat, A., Ludwig, W., Verdoit-Jarraya, M., Heussner, S.,
855 Canals, M., 2014. Biogeochemical characterization of the riverine particulate organic matter
856 transferred to the NW Mediterranean Sea. Biogeosciences 11, 157–172.
857 https://doi.org/10.5194/bg-11-157-2014

858 Husson, F., Josse, J., Pages, J., 2010. Principal component methods-hierarchical clustering-partitional
859 clustering: why would we need to choose for visualizing data? Applied Mathematics
860 Department.
861 Jennerjahn, T.C., Ittekkot, V., 1997. Organic matter in sediments in the mangrove areas and adjacent
862 continental margins of Brazil: I. Amino acids and hexosamines. Oceanologica Acta 20, 359–369.
863 Lansard, B., Rabouille, C., Denis, L., Grenz, C., 2008. In situ oxygen uptake rates by coastal sediments
864 under the influence of the Rhone River (NW Mediterranean Sea). Continental Shelf Research
865 28, 1501–1510. https://doi.org/10.1016/j.csr.2007.10.010
866 Lê, S., Josse, J., Husson, F., 2008. FactoMineR: An R Package for Multivariate Analysis | Lê | Journal of
867 Statistical Software 25, 1–18. https://doi.org/10.18637/jss.v025.i01
868 Leithold, E.L., Hope, R.S., 1999. Deposition and modification of a flood layer on the northern California
869 shelf: lessons from and about the fate of terrestrial particulate organic carbon. Marine Geology
870 154, 183–195.
871 Li, Y., Gregory, S., 1974. Diffusion of Ions in Sea-Water and in Deep-Sea Sediments. Geochimica et
872 Cosmochimica Acta 38, 703–714.
873 Lindroth, P., Mopper, K., 1979. High performance liquid chromatographic determination of subpicomole
874 amounts of amino acids by precolumn fluorescence derivatization with ortho-phthaldialdehyde.
875 Analytical Chemistry 51, 1667–1674.
876 Lohrer, A.M., Thrush, S.F., Hewitt, J.E., Berkenbusch, K., Ahrens, M., Cummings, V.J., 2004. Terrestrially
877 derived sediment: response of marine macrobenthic communities to thin terrigenous deposits.
878 Marine Ecology Progress Series 273, 121–138. https://doi.org/10.3354/meps273121
879 Lorthiois, T., 2012. Dynamique des matières en suspension dans le panache du Rhône (Méditerranée
880 occidentale) par télédétection spatiale “couleur de l’océan” (thesis). Université Paris 6.
881 Maillet, G.M., Vella, C., Berné, S., Friend, P.L., Amos, C.L., Fleury, T.J., Normand, A., 2006. Morphological
882 changes and sedimentary processes induced by the December 2003 flood event at the present
883 mouth of the Grand Rhône River (southern France). Marine Geology 234, 159–177.

884 Maria, T.F., Vanaverbeke, J., Esteves, A.M., De Troch, M., Vanreusel, A., 2012. The importance of
885 biological interactions for the vertical distribution of nematodes in a temperate ultra-dissipative
886 sandy beach. Estuarine, Coastal and Shelf Science 97, 114–126.
887 https://doi.org/10.1016/j.ecss.2011.11.030
888 Marion, C., Maillet, G., Arnaud, M., Eyrolle, F., 2010. Quantifications des flux solides rhôdaniens à
889 l'embouchure: apports de la Durance pendant la crue exceptionnelle de mai 2008. La Houille
890 Blanche 72–80. https://doi.org/10.1051/lhb/2010057
891 Martin, D., Pititto, F., Gil, J., Mura, M.P., Bahamon, N., Romano, C., Thorin, S., Schvartz, T., Dutrieux, É.,
892 Bocquenet, Y., 2019. Long-distance influence of the Rhône River plume on the marine benthic
893 ecosystem: Integrating descriptive ecology and predictive modelling. Science of The Total
894 Environment 673, 790–809. https://doi.org/10.1016/j.scitotenv.2019.04.010
895 Mayer, L.M., Schick, L.L., Sawyer, T., Plante, C.J., Jumars, P.A., Self, R.L., 1995. Bioavailable amino acids
896 in sediments: a biomimetic, kinetics-based approach. Limnology and Oceanography 40, 511–
897 520.
898 Meyers, P.A., 1997. Organic geochemical proxies of paleoceanographic, paleolimnologic, and
899 paleoclimatic processes. Organic Geochemistry 27, 213–250.
900 Moens, T., Braeckman, U., Derycke, S., Fonseca, G., Gallucci, F., Ingels, J., Leduc, D., Vanaverbeke, J., Van
901 Colen, C., Vanreusel, A., Vincx, M., 2013. Ecology of free-living marine nematodes, in: Handbook
902 of Zoology: Gastrotricha, Cycloneuralia and Gnathifera, Vol. 2 : Nematoda. De Gruyter, pp. 109–
903 152.
904 Mojtahid, M., Jorissen, F., Lansard, B., Fontanier, C., 2010. Microhabitat selection of benthic
905 foraminifera in sediments off the Rhöne River mouth (NW Mediterranean). Journal of
906 Foraminiferal Research 40, 231–246. https://doi.org/10.2113/gsjfr.40.3.231
907 Mojtahid, M., Jorissen, F., Lansard, B., Fontanier, C., Bombled, B., Rabouille, C., 2009. Spatial distribution
908 of live benthic foraminifera in the Rhône prodelta: faunal response to a continental-marine

organic matter gradient. Marine Micropaleontology 70, 177–200. https://doi.org/10.1016/j.marmicro.2008.12.006

Moloney, C.L., Field, J.G., 1991. The size-based dynamics of plankton food webs. I. A simulation model of carbon and nitrogen flows. Journal of Plankton Research 13, 1003–1038. https://doi.org/10.1093/plankt/13.5.1003

Moodley, L., Chen, G., Heip, C.H.R., Vincx, M., Ecosystems Studies, 2000. Vertical distribution of meiofauna in sediments from contrasting sites in the Adriatic Sea: Clues to the role of abiotic versus biotic control. Ophelia 53, 203–212. https://doi.org/10.1080/00785326.2000.10409450

Motoda, S., 1959. Devices of simple plankton apparatus. Memoirs of the Faculty of Fisheries, Hokkaido University, 7(1-2), 73-9.

Norkko, A., Thrush, S.F., Hewitt, J.E., Cummings, V.J., Norkko, J., Ellis, J.I., Funnell, G.A., Schultz, D., MacDonald, I., 2002. Smothering of estuarine sandflats by terrigenous clay: the role of wind-wave disturbance and bioturbation in site-dependent macrofaunal recovery. Marine Ecology Progress Series 234, 23–42. https://doi.org/10.3354/meps234023

Oksanen, J., Blanchet, F.G., Friendly, M., Kindt, R., Legendre, P., McGlinn, D., Minchin, P.R., O'Hara, R.B., Simpson, G.L., Solymos, P., Henry, M., Stevens, H., E Szoecs, Wagner, H., 2016. vegan: Community Ecology Package. CRAN: The Comprehensive R Archive Network.

O'Leary, J.K., Micheli, F., Airoldi, L., Boch, C., De Leo, G., Elahi, R., Ferretti, F., Graham, N.A.J., Litvin, S.Y., Low, N.H., Lummis, S., Nickols, K.J., Wong, J., 2017. The Resilience of Marine Ecosystems to Climatic Disturbances. BioScience 67, 208–220. https://doi.org/10.1093/biosci/biw161

Olivier, J.-M., Dole-Olivier, M.-J., Amoros, C., Carrel, G., Malard, F., Lamouroux, N., Bravard, J.-P., 2009. Chapter 7 - The Rhône River Basin, in: Tockner, K., Uehlinger, U., Robinson, C.T. (Eds.), Rivers of Europe. Academic Press, London, pp. 247–295. https://doi.org/10.1016/B978-0-12-369449-2.00007-2

933 Palacín, C., Gili, J.-M., Martín, D., 1992. Evidence for coincidence of meiofauna spatial heterogeneity
934 with eutrophication processes in a shallow-water Mediterranean bay. Estuarine, Coastal and
935 Shelf Science 35, 1–16. https://doi.org/10.1016/S0272-7714(05)80053-8
936 Palmer, M.A., Gusf, G., 1985. Dispersal of meiofauna in a turbulent tidal creek. Journal of Marine
937 Research 43, 179–210. https://doi.org/10.1357/002224085788437280
938 Palmer, M.A., Montagna, P.A., Spies, R.B., Hardin, D., 1988. Meiofauna dispersal near natural petroleum
939 seeps in the Santa Barbara channel: A recolonization experiment. Oil and Chemical Pollution 4,
940 179–189.
941 Pastor, L., Deflandre, B., Viollier, E., Cathalot, C., Metzger, E., Rabouille, C., Escoubeyrou, K., Lloret, E.,
942 Pruski, A.M., Vétion, G., Desmalades, M., Buscail, R., Grémare, A., 2011a. Influence of the
943 organic matter composition on benthic oxygen demand in the Rhône River prodelta (NW
944 Mediterranean Sea). Continental Shelf Research 31, 1008–1019.
945 https://doi.org/10.1016/j.csr.2011.03.007
946 Pastor, L., Rabouille, C., Metzger, E., Thibault de Chanvalon, A., Viollier, E., Deflandre, B., 2018. Transient
947 early diagenetic processes in Rhône prodelta sediments revealed in contrasting flood events.
948 Continental Shelf Research 166, 65–76. https://doi.org/10.1016/j.csr.2018.07.005
949 Payrastre, O., Naulin, J.P., Nguyen, C.C., Gaume, E., 2012. Analyse hydrologique des crues de juin 2010
950 dans le Var (Rapport de recherche). IFSTTAR - Institut Français des Sciences et Technologies des
951 Transports, de l'Aménagement et des Réseaux.
952 Pelletier, É., Deflandre, B., Nozais, C., Tita, G., Desrosiers, G., Gagné, J.-P., Mucci, A., 1999. Crue éclair
953 de juillet 1996 dans la région du Saguenay (Québec). 2. Impacts sur les sédiments et le biote de
954 la baie des Ha! Ha! et du fjord du Saguenay. Canadian Journal of Fisheries and Aquatic Sciences.
955 56, 2136–2147. https://doi.org/10.1139/f99-143
956 Pont, D., Simonnet, J.-P., Walter, A.V., 2002. Medium-term Changes in Suspended Sediment Delivery to
957 the Ocean: Consequences of Catchment Heterogeneity and River Management (Rhône River,
958 France). Estuarine, Coastal and Shelf Science 54, 1–18. https://doi.org/10.1006/ecss.2001.0829

959 Pruski, A.M., Buscail, R., Bourgeois, S., Vétion, G., Coston-Guarini, J., Rabouille, C., 2015.
960 Biogeochemistry of fatty acids in a river-dominated Mediterranean ecosystem (Rhône River
961 prodelta, Gulf of Lions, France): Origins and diagenesis. Organic Geochemistry 83–84, 227–240.
962 https://doi.org/10.1016/j.orggeochem.2015.04.002
963 Rabouille, C., 2010a. MESURHOBENT 1 cruise,Téthys II R/V. https://doi.org/10.17600/10450020
964 Rabouille, C., 2010b. MESURHOBENT 2 cruise,Téthys II R/V. https://doi.org/10.17600/10450060
965 Rabouille, C., 2010c. MESURHOBENT 3 cruise,Téthys II R/V. https://doi.org/10.17600/10450100
966 Rabouille, C., 2010d. MESURHOBENT 4 cruise,Téthys II R/V. https://doi.org/10.17600/10450140
967 Rabouille, C., Denis, L., Dedieu, K., Stora, G., Lansard, B., Grenz, C., 2003. Oxygen demand in coastal
968 marine sediments: comparing in situ microelectrodes and laboratory core incubations. Journal
969 of Experimental Marine Biology and Ecology 285–286, 49–69. https://doi.org/10.1016/S0022-
970 0981(02)00519-1
971 Rassmann, J., Eitel, E.M., Lansard, B., Cathalot, C., Brandily, C., Taillefert, M., Rabouille, C., 2020. Benthic
972 alkalinity and dissolved inorganic carbon fluxes in the Rhone River prodelta generated by
973 decoupled aerobic and anaerobic processes. Biogeosciences 17, 13–33.
974 https://doi.org/10.5194/bg-17-13-2020
975 Riera, P., Hubas, C., 2003. Trophic ecology of nematodes from various microhabitats of the Roscoff Aber
976 Bay (France): importance of stranded macroalgae evidenced through δ13C and δ15N. Marine
977 Ecology Progress Series 260, 151–159. https://doi.org/10.3354/meps260151
978 Rudnick, D., 1989. Time lags between the deposition and meiobenthic assimilation of phytodetritus.
979 Marine Ecology Progress Series 50, 231-240. https://doi.org/10.3354/meps050231
980 Salen-Picard, C., Arlhac, D., Alliot, E., 2003. Responses of a Mediterranean soft bottom community to
981 short-term (1993-1996) hydrological changes in the Rhône river. Marine Environmental
982 Research 55, 409–427.
983 Schratzberger, M., Ingels, J., 2018. Meiofauna matters: The roles of meiofauna in benthic ecosystems.
984 Biology and Ecology 502, 125-25.

985 Schratzberger, M., Whomersley, P., Warr, K., Bolam, S.G., Rees, H.L., 2004. Colonisation of various types
986 of sediment by estuarine nematodes via lateral infaunal migration: a laboratory study. Marine
987 Biology 145, 69–78. https://doi.org/10.1007/s00227-004-1302-1
988 Scott, D.B., Tobin, R., Williamson, M., Medioli, F.S., Latimer, J.S., Boothman, W.A., Asioli, A., Haury, V.,
989 2005. Pollution monitoring in two North American estuaries: historical reconstructions using
990 benthic foraminifera. Journal of Foraminiferal Research 35, 65–82.
991 https://doi.org/10.2113/35.1.65
992 Semprucci, F., Balsamo, M., Appolloni, L., Sandulli, R., 2018. Assessment of ecological quality status
993 along the Apulian coasts (eastern Mediterranean Sea) based on meiobenthic and nematode
994 assemblages. Mar Biodiv 48, 105–115. https://doi.org/10.1007/s12526-017-0745-9
995 Semprucci, F., Facca, C., Ferrigno, F., Balsamo, M., Sfriso, A., Sandulli, R., 2019. Biotic and abiotic factors
996 affecting seasonal and spatial distribution of meiofauna and macrophytobenthos in transitional
997 coastal waters. Estuarine, Coastal and Shelf Science, 219, 328–340.
998 https://doi.org/10.1016/j.ecss.2019.02.008
999 Shimanaga, M., Kitazato, H., Shirayama, Y., 2000. Seasonal Patterns of Vertical Distribution between
1000 Meiofaunal Groups in Relation to Phytodetritus Deposition in the Bathyal Sagami Bay, Central
1001 Japan. Journal of Oceanography 56, 379–387. https://doi.org/10.1023/A:1011120204419
1002 Soetaert, K., Vincx, M., Wittoeck, J., Tulkens, M., 1995. Meiobenthic distribution and nematode
1003 community structure in five European estuaries. Hydrobiologia 311, 185–206.
1004 https://doi.org/10.1007/BF00008580
1005 ter Braak, C.J.F., 1986. Canonical Correspondence Analysis: A New Eigenvector Technique for
1006 Multivariate Direct Gradient Analysis. Ecology 67, 1167–1179.
1007 https://doi.org/10.2307/1938672
1008 Tesi, T., Langone, L., Goñi, M.A., Miserocchi, S., Bertasi, F., 2008. Changes in the composition of organic
1009 matter from prodeltaic sediments after a large flood event (Po River, Italy). Geochimica et
1010 Cosmochimica Acta 72, 2100–2114. https://doi.org/10.1016/j.gca.2008.02.005

1011 Ulses, C., Estournel, C., Durrieu de Madron, X., Palanques, A., 2008. Suspended sediment transport in
1012 the Gulf of Lions (NW Mediterranean): Impact of extreme storms and floods. Continental Shelf
1013 Research 28, 2048–2070. https://doi.org/10.1016/j.csr.2008.01.015
1014 Vanaverbeke, J., Steyaert, M., Soetaert, K., Rousseau, V., Van Gansbeke, D., Parent, J.-Y., Vincx, M., 2004.
1015 Changes in structural and functional diversity of nematode communities during a spring
1016 phytoplankton bloom in the southern North Sea. Journal of Sea Research 52, 281–292.
1017 https://doi.org/10.1016/j.seares.2004.02.004
1018 Vanreusel, A., Vincx, M., Schram, D., Gansbeke, D. van, 1995. On the Vertical Distribution of the
1019 Metazoan Meiofauna in Shelf Break and Upper Slope Habitats of the NE Atlantic. Internationale
1020 Revue der gesamten Hydrobiologie und Hydrographie 80, 313–326.
1021 https://doi.org/10.1002/iroh.19950800218
1022 Villora-Moreno, S., 1997. Environmental Heterogeneity and the Biodiversity of Interstitial Polychaeta.
1023 Bulletin of Marine Science 60, 494–501.
1024

Table 1: Principal descriptors used in this study with their interpretation.

Descriptors	Feature	Main diagnostic information	References
C/N	Source/Quality	Marine derived OM (6-9), Soil derived OM (8-20) and higher plants (>20); may decrease during OM decomposition	Moloney and Field (1991), Hedges and Oades (1997), Meyers (1997)
$\delta^{13}C$	Source	Marine OM (−20.1±0.8‰) and Rhône River inputs (−27.1 ± 0.6‰)	Harmelin-Vivien et al. (2008) and Higueras et al. (2014)
DI	Quality	Diagenetic alteration of OM with DI values ranging from −2.2 extensively degraded sediments to -1.5 for fresh algae	Dauwe et al. (1999b)
RI	Quality	Selective degradation during diagenesis and production of non-proteic amino acids, lower values in degraded sediments	Jennerjahn & Ittekkot (1997)
EHAA/THAA (%)	Quality	OM bioavailability for the benthic fauna ranging from 0 to 100%	Mayer et al. (1995)
MC-SAFA	Source	Mixed origin, but shorter chains predominate in phytoplankton	Dunstan et al. (1994), Bianchi and Canuel (2011)
LC-SAFA	Source	Terrestrial higher plants, macrodetritus	Bianchi and Canuel (2011), Dunstan et al. (1994), Pruski et al. (2015)
Ter PUFA	Source	Terrestrial higher plants (>2.5%)	Budge et al. (2001), Pruski et al. (2015)
Algal PUFA	Source	Phytoplankton with $C_{20:5\omega3}$ specific of diatoms	Dunstan et al. (1994)
MUFA	Source	Mixed origin with $C_{16:1\omega7}$ common in diatoms and bacteria	Bianchi and Canuel (2011), Dunstan et al. (1994)
BAFA	Source	Bacterial sources	Bianchi and Canuel (2011)

The degradation index (DI), reactivity index (RI) and enzymatically hydrolysable amino acids to total hydrolysable amino acids ratio (EHAA/THAA) are inferred from the amino acid composition. Fatty acid biomarkers are grouped as follows: mid-chain even-number saturated fatty acids with less than 20 carbons (MC-SAFAs), long-chain saturated fatty acids with 24 carbon or more (LC-SAFA), polyunsaturated fatty acids with 18 carbons ($C_{18:2\omega6}$ and $C_{18:3\omega3}$, Terr PUFA), the remaining PUFA attributed to microalgae (Algal PUFA), the monounsaturated fatty acids (MUFA) and the straight and branched odd-numbered fatty acids of bacterial origin (BAFA). The unsaturation index is calculated as the sum of products of the number of double bonds of each acid multiplied by its percentage of the total fatty acid composition.

Table 2: Temporal variations of Diffusive Oxygen Uptake (DOU) rates in the sediments of the Rhône River prodelta in April, July and August 2010. Values are means ± standard deviations (n= 4), nd= not determined.

Stations	DOU		
	April 2010	**July 2010**	**August 2010**
MESURHO	16.9 ± 4.1	10.1 ± 0.6	9 ± 1.5
A	14.9 ± 1.3	10.6 ± 3.6	nd
AK	19.7 ± 3.5	11.4 ± 1.3	nd
B	12.7 ± 2.1	11.3 ± 2.9	nd
K	14.9 ± 2.6	11.8 ± 4.9	nd

Table 3: Marginal and conditional effects of environmental variables determined using forward selection. Ranking is based on their P-value and Akaike Information Criterion (AIC) where the variable with the lowest AIC value is the most influential. 999 permutations. Significant variables are indicated in bold, * p<0.05, ** p<0.01. Best combination of variables: Porosity + $\delta^{13}C$ + DI.

Marginal effects						Conditional effects					
Rank	**Variable**	**AIC**	**F ratio**	**Pr(>F)**		**Rank**	**Variable**	**AIC**	**F ratio**	**Pr(>F)**	
1	**Porosity**	79.935	7.267	0.005	**	1	**Porosity**	79.935	7.267	0.005	**
2	**Algal PUFA**	81.865	5.0518	0.005	**	2	**$\delta^{13}C$**	78.509	3.2544	0.015	*
3	**EHAA**	81.042	5.9774	0.015	**	3	**DI**	77.785	2.4517	0.045	*
4	C/N	85.621	1.1536	0.270		-	EHAA	78.170	1.3657	0.180	
5	$\delta^{13}C$	85.715	1.0625	0.385		-	Clay	78.285	1.2658	0.290	
6	EHAA/THAA	86.120	0.6742	0.575		-	Algal PUFA	78.507	1.0746	0.400	
7	DI	86.174	0.6229	0.605		-	EHAA/THAA	79.305	0.3983	0.795	
8	$CaCO_3$	86.252	0.5482	0.655		-	$CaCO_3$	79.301	0.4013	0.820	
9	Clay	86.343	0.4626	0.715		-	C/N	79.419	0.303	0.925	